RSC Applied Interfaces

ROYAL SOCIETY OF CHEMISTRY

REVIEW

View Article Online
View Journal

Cite this: DOI: 10.1039/d5lf00077g

Zinc-ion batteries: pioneering the future of sustainable energy storage through advanced materials and mechanisms

Zixuan Chen,†[a] Liang Zhang,†[c] Tianyu Yu,[f] Huancheng Yang,[a] Yao Lu, *[b] Xiaodan Wang,*[d] Rui Li,*[e] Zonglun Ye,[g] Yue Wang,[d] Pengwei Li,[d] Bowen Zheng,[hj] Yukun Sun,[i] Depeng Wang,[i] Guoqiang Xu[i] and Wenchao Gao*[b]

The growing global demand for sustainable energy storage has positioned zinc-ion batteries (ZIBs) as a promising alternative to lithium-ion batteries (LIBs), offering inherent advantages in safety, cost, and environmental compatibility. Despite challenges like dendrite formation and cathode dissolution, recent advancements in electrode materials and electrolytes show significant progress. Anode innovations focus on surface modification and structural engineering to mitigate dendrites, while cathode development explores manganese/vanadium oxides, Prussian blue analogs, and emerging materials like Chevrel phases and MXenes. Electrolyte optimization, including aqueous, non-aqueous, and hybrid systems, has improved ion transport and interfacial stability. Mechanistic studies reveal complex redox processes involving cations, anions, and functional groups, guiding material design. ZIBs demonstrate potential for grid storage, flexible electronics, and electric vehicles, though challenges in energy density and cycle life remain. Addressing these through advanced characterization, computational modeling, and scalable fabrication could accelerate ZIB commercialization, establishing them as key players in sustainable energy storage and supporting global decarbonization efforts. Future research should focus on interdisciplinary approaches to overcome existing limitations and unlock their full potential. This review consolidates current knowledge while outlining pathways for ZIB development toward practical implementation.

Received 18th March 2025,
Accepted 1st July 2025

DOI: 10.1039/d5lf00077g

rsc.li/RSCApplInter

1. Introduction

In the quest for carbon neutrality, energy storage technologies are increasingly recognized as essential to building a sustainable energy ecosystem. The transition from fossil fuels to renewable sources such as wind and solar requires efficient and scalable storage solutions to handle their inherent intermittency.

LIBs, currently the backbone of the energy storage market, have facilitated the proliferation of electric vehicles, the construction of smart grids, and the evolution of portable electronic devices with their high energy density, long cycle life, and wide range of applications. Regardless of the notable benefits offered by LIBs, such as their impressive capacity, durability, and efficiency, their associated shortcomings including safety issues, environmental concerns, and shortage of raw materials are unneglectable problems. In tandem with the aggressive surge in energy density over the past decade, incidents stemming from LIBs have assumed greater significance. These accidents result from inadvertent chemical energy release, potentially leading to substantial property loss and, in some cases, even posing threats to human life.[1–3] Furthermore, the disposal of LIBs can give rise to significant environmental issues, including the destruction of ecosystems and the highly polluting processes involved in metal extraction.[4] The unregulated extraction of critical components like lithium, cobalt, and nickel, which are

[a] School of Mechanical Engineering, University of Shanghai for Science and Technology, Shanghai 200093, P. R. China
[b] CAS Center for Excellence in Nanoscience, Beijing Key Laboratory of Micro-Nano Energy and Sensor, Beijing Institute of Nanoenergy and Nanosystems, Chinese Academy of Sciences, Beijing 101400, P. R. China. E-mail: Luyao@binn.cas.cn
[c] College of Physics and Mathematics and Beijing Key Laboratory for Magneto-Photoelectrical Composite and Interface Science, University of Science and Technology Beijing, Beijing 100083, P. R. China
[d] China Astronaut Research and Training Center, Beijing 100094, P. R. China
[e] Beijing Key Laboratory of Environmental, Science and Engineering School of Materials Science & Engineering Beijing Institute of Technology, Beijing 100081, P. R. China
[f] Shanghai Suochen Information Technology Co., Ltd., Shanghai 200030, P. R. China
[g] Capital University of Economics and Business, Beijing 100070, P. R. China
[h] Ordos New Energy Research Institute, Ordos 017000, Inner Mongolia, P. R. China
[i] Sichuan New Energy Vehicle Innovation Center, Co., Ltd., Yibin 644000, Sichuan, P. R. China
[j] State Key Laboratory of Intelligent Green Vehicle and Mobility, School of Vehicle and Mobility, Tsinghua University, Beijing 100084, P. R. China
† Z. C. and L. Z. contributed equally to this paper.

integral to LIBs, exacerbates the scarcity of these naturally limited metals. This, in turn, is likely to result in foreseeable spikes in raw material prices and intensify competition for these resources. As society's pursuit of cleaner energy and a lower-carbon lifestyle intensifies, the high carbon emissions associated with the production, usage, and recycling of LIBs have gradually come into focus, prompting the search for more environmentally friendly and efficient energy storage solutions. Thus, although LIBs currently dominate the market, their limitations including safety issues, limited resources, and high costs have driven the exploration of alternative technologies.

In view of this dilemma, rechargeable aqueous zinc-ion batteries (ZIBs) have gained attention for their enhanced safety, sustainability, and cost-effectiveness. Specifically, zinc is a kind of abundant element in the Earth's crust, and its extraction and processing would be both economically viable and environmentally favorable, with notably lower carbon emissions compared to the extraction and refinement of lithium. This intrinsic advantage results in a lower carbon footprint for ZIBs from the outset. Moreover, the manufacturing process of ZIBs is simpler and less energy-intensive compared to the complex production chain of LIBs, thereby further reducing energy consumption and associated emissions. This streamlined production not only enhances the environmental friendliness of ZIBs but also supports a significant reduction in carbon emissions across the entire industrial supply chain. Besides, ZIBs demonstrate superior stability and safety during cycling, which helps to minimize carbon emissions associated with battery failures or premature retirements. These attributes collectively position ZIBs as a promising low-carbon alternative in the field of energy storage, supporting the transition to more sustainable energy systems.[5–8]

However, ZIBs have encountered obstacles that hinder their practical application such as dendrite growth, limited voltage window and possible corrosion reaction.[8–11] To overcome these issues, recent research has focused on electrode materials regulation and electrolyte optimization. With regard to the anode side, initiatives are concentrated on growth control, structural design, and additives selection, aiming for alleviating dendrite formation and enhancing plating/stripping coulombic efficiency. Concerning the cathode aspect, efforts focus on regulation of electronic structure, optimization of crystal structure, defect engineering, and control of microstructure. Meanwhile, development of electrolytes has led to products with excellent Zn^{2+} conductivity and highly reversible Zn stripping/plating behavior.[12,13] Organic,[14] ionic liquids,[15] aqueous,[16] and solid-state[17] electrolytes have made significant strides in recent years, these advancements are crucial for enhancing the safety, energy density, and overall performance of ZIBs.[18]

In addition to the development of components for ZIBs, research on the actual operating mechanisms would be crucial as well.[19] It aids in more effectively investigating the failure mechanism during the service life, enabling the design of enhanced electrochemical performance. Recent advances in characterization techniques have offered unprecedented opportunities to investigate the electrochemical reaction of ZIBs. In particular, *in situ* characterization techniques can provide real-time observations of the structural and electronic changes during the charge/discharge process.[20–26]

Despite the significant advancements, several challenges remain in the journey towards the commercialization of ZIBs. For instance, the practical energy density of ZIBs is still lower than that of LIBs, which is mainly due to the sluggish kinetics of Zn^{2+} insertion/extraction.[27–30] Additionally, while ZIBs have been proposed for various applications including grid-scale energy storage, portable electronics, flexible or wearable devices, and electric vehicles, but their widespread adoption necessitates further improvements in cycle life, energy density, and power density.[31] Furthermore, to realize the full potential of ZIBs, more effort should be devoted to fundamental research,[30,32] for instance, unraveling the intrinsic process of Zn ions storage in various host materials

Yao Lu

Yao Lu completed his MS and PhD degrees at the University of Science and Technology Beijing in 2020. Then he joined the State Key Laboratory of Automotive Safety and Energy at Tsinghua University as an assistant research fellow. Now, he is appointed as an Associate Researcher in Beijing institute of nanoenergy and nanosystems, Chinese Academy of Sciences. His research interest is smart batteries based on implanted flexible sensors.

Wenchao Gao

Wenchao Gao received PhD from the Monash University in 2020. He is currently a professor and a group leader at Beijing Institute of Nanoenergy and Nanosystems, Chinese Academy of Sciences (CAS). Wenchao has worked for more than 5 years in the areas of nanomaterials design/characterization, multi-scale coupled numerical modelling and experimental validation on electrohydrodynamic, corona discharge, particle charging and particle trajectories, and mechanics of structures.

holds significance, because the understanding of the reaction mechanism at the atomic or molecular level is the key to guide the rational design of better materials.[33] In addition, the accelerated discovery and development of novel materials *via* high-throughput computational methods and machine learning could be game-changers in the field.[34,35] Although ZIBs are attracting increasing attention, it is imperative to thoroughly understand the advantages and limitations of the technology. With the continuous development of materials, electrolytes, and cell designs, coupled with a deep understanding of the operating mechanisms, ZIBs could indeed provide a viable and competitive alternative to current battery technologies in the foreseeable future.

At present, aqueous ZIBs still face enormous challenges such as low energy density and short cycle life. There is an urgent need to continue to strengthen basic research and technology development in this field. Focusing on the basic scientific issues existing in aqueous ZIBs, this paper systematically summarizes the latest progress of anode materials, cathode materials, electrochemical mechanism and electrolyte design for aqueous ZIBs, as well as their respective core issues and research strategies, as shown in Fig. 1. Additionally, we provide an evaluation of potential application avenues and projected market growth for ZIBs with a particular emphasis on their prospective commercialization and deployment in stationary energy resources. Through presenting this comprehensive review, our aim is to offer an up-to-date perspective on the current status and future directions of ZIB technology.

2. Anode electrode of ZIBs

The design and optimization of anode materials are pivotal in advancing the performance metrics of ZIBs. An ideal anode material must exhibit a combination of high electrical conductivity, fast zinc-ion diffusion kinetics, and a structurally stable framework capable of mitigating issues related to volume expansion and morphological degradation during repeated charge–discharge cycles. According to the electrochemical behavior of Zn^{2+} in the charge and discharge processes, the anode materials can be roughly classified into two categories: (1) materials that can demonstrate Zn^{2+} stripping/plating behavior, such as metal Zn anode, which would be widely utilized and (2) materials with Zn^{2+} intercalation behavior.[36]

2.1. Metal Zn anode

Metallic zinc is a common choice for ZIB anode due to the high theoretical capacity and low redox potential.[37] However, the actual application process is fraught with numerous issues such as Zn dendrites,[38] corrosion,[39,40] and passivation.[41]

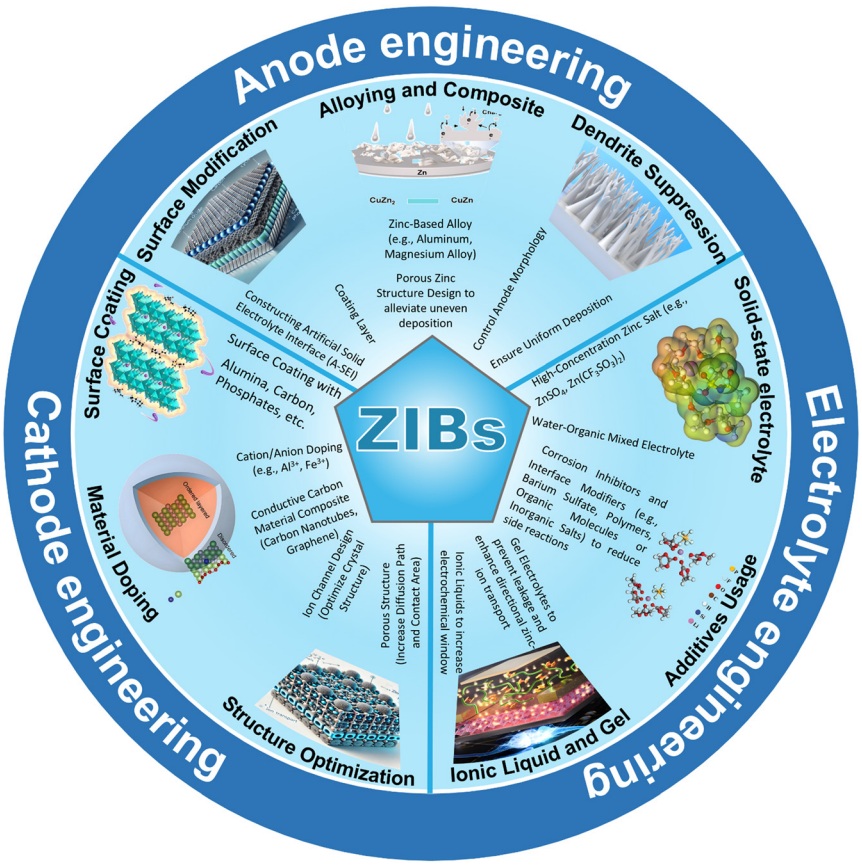

Fig. 1 Development and strategies of ZIBs in anode, cathode, and electrolyte.

In aqueous ZIBs, zinc dendrite growth is a complex process. During charging, zinc ions migrate and deposit on the electrode surface under the influence of an electric field. Due to surface irregularities, zinc ions preferentially deposit in certain areas, forming initial zinc nuclei. As deposition continues, zinc atoms accumulate and diffuse, leading to the formation of dendritic structures. The growth of these dendrites is influenced by factors such as electric field distribution, ion concentration gradients, current density, and electrolyte composition. The uneven growth of dendrites may cause short circuits, reduce coulombic efficiency, and pose safety risks. Thus, inhibiting dendrite growth is crucial for enhancing the performance and safety of ZIBs.[42]

As for corrosion of Zn metal, it mainly occurs during the electrochemical reaction. When Zn sheds electrons, it transforms into Zn^{2+}, eventually dissolving in the electrolyte upon the discharge process. The hydrogen evolution reactions would elevate the concentration of OH^- locally and lead to the formation of insoluble compounds (Zn oxides and hydroxides in neutral or slightly alkaline solutions and zincate ions in high pH (pH $>$ 9) solutions) throughout the charging process. Moreover, as dendrites grow, the surface area of the Zn anode grows. This growth is further intensified by the corrosion reaction, leading to an accelerated depletion of the Zn anode and declining battery efficiency.[36,43,44]

Besides, the issue of passivation on the surface demands attention and cannot be overlooked. The byproducts resulting from the detrimental interaction of Zn^{2+} and OH^- would induce passivation on the Zn surface, influencing dissolution of Zn anode and the movement of carriers. The process of passivation creates a protective layer on the electrode's surface, which inhibits the release of discharge products and/or OH^-, preventing further discharge. As the discharge products attains its maximum solubility during the discharge, ZnO would form as precipitate on the electrode's surface. Pore dimensions in porous Zn electrodes diminish due to the precipitation of ZnO prior to passivation. As soon as the newly released discharge products significantly surpasses the solubility threshold, it promptly precipitates, which can fully obstruct the residual pore space, leading to passivation.[45–47]

In response to these issues, numerous scientists have conducted thorough investigations into preparing advanced Zn anodes, which can be summarized as three main design strategies as following:

(1) Surface modification. Altering the surface of Zn proves to be an efficient method for the establishment of high-efficiency Zn anodes. The surface modification aims to guarantee even deposition of Zn through the engineered artificial interface layer, facilitating consistent Zn nucleation and a flat deposition layer, as opposed to coarse-grained matter. Through this method, the growth of zinc dendrites can be significantly reduced, along with potential corrosion and passivation during battery service.[9,53] Yang *et al.*[48] utilized metal–organic framework (MOF) to create a protective surface layer that maintained a supersaturated electrolyte on the Zn anode (Fig. 2a). The innovation resulted in symmetric Zn cells exhibiting an exceptional lifespan of

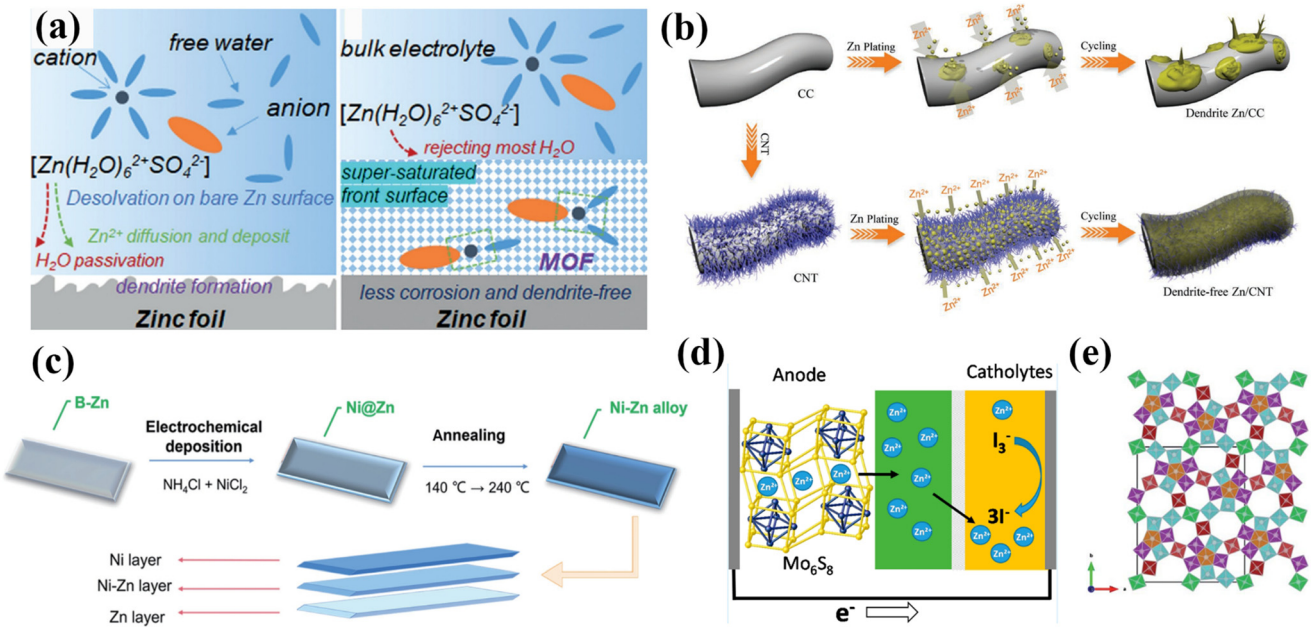

Fig. 2 (a) Schematic illustration of the surface evolution of Zn. Reproduced with permission from ref. 48. Copyright 2020, WILEY-VCH Verlag GmbH & Co. KGaA, Weinheim. (b) The schematic illustrations of Zn deposition on CC and CNT electrodes. Reproduced with permission from ref. 49. Copyright 2019, WILEY-VCH Verlag GmbH & Co. KGaA, Weinheim. (c) Schematic illustration of fabrication procedure and mechanism simulations of Ni–Zn alloy. Reproduced with permission from ref. 50. Copyright 2023, Springer. (d) Mo_6S_8 for anode in ZIBs. Reproduced with permission from ref. 51. Copyright 2016, American Chemical Society. (e) $Mo_{2.5+y}VO_{9+z}$ host framework. Reproduced with permission from ref. 52. Copyright 2016, Royal Society of Chemistry.

3000 hours at 0.5 mA cm^{-2}, approximately 55 times longer than bare Zn anodes, while also improving the Zn electrodeposit morphology and enabling high-performance aqueous MnO_2–Zn batteries with notable reversible capacity and stability. Besides, modifying zinc anode with carbon-based materials,[54] inorganic nonmetallic materials,[55] polymer materials,[56] metallic materials,[57] or composite material[58] would also achieve the effective protection of Zn anode to a certain extent, so as to achieve the purpose of improving the life and electrochemical performance.

(2) Structural design. In aqueous ZIBs, the purpose of structural optimization aims to decelerate the change in shape and formation of Zn dendrites, thereby diminishing internal resistance and averting the irregular distribution of Zn ions on the anode surface caused by the growth of dendrites.[59]

Lately, extensive research has been conducted on creating viable methods for structuring three-dimensional Zn anodes, which is capable of enlarging the Zn anode's surface area and diminishing the overpotential in Zn deposition, thereby decreasing the chances of dendrite development and passivation.[60,61] Parker *et al.*[62] developed a 3D porous sponge Zn electrode, which enhances Zn utilization and charging capacity, and this design enlarges the active area and diminishes the local current density, thereby mitigating Zn dendrite formation. Besides, Zn can be also capable of being applied as an active material to deposited on different base materials with a certain spatial configuration. Zeng *et al.*[49] achieved dendrites-free Zn anodes by incorporating a 3D structure of carbon nanotubes (CNTs) into the surface of a carbon cloth substrate (CC) to serve as a scaffold for Zn plating and stripping (Fig. 2b). In contrast to the pristine deposited Zn electrode, the as-fabricated anode affords lower overpotential for Zn nucleation and more homogeneously distributed electric field, making it more favorable for highly reversible Zn plating/stripping with satisfactory coulombic efficiency rather than the formation of Zn dendrites or other byproducts. Besides, metal-based materials,[63] MOF materials,[64] and 2D MXene[65] can be good choices for Zn depositing as well.

(3) Zn alloying. Alloying would be a common method for stabilizing the cycling performance of metal anodes. At present, the techniques for Zn alloying can be generally categorized into two main types. One involves blending zinc with other metallic elements and then rolling the mixture to produce the desired zinc alloy strips, during which the Zn-based alloy phase can be formed. Wang and his co-workers[66] presented a lamella-nanostructured $Zn_{88}Al_{12}$ alloy based on the eutectic alloying strategy, significantly enhancing the electrochemical performance when used as dendrite-free and reversible anode for ZIBs. The other method would be more familiar, which involves electroplating or other techniques, such as thermal evaporation, atomic layer deposition, magnetron sputtering, and chemical conversion, aiming to introduce a wider range of elements to directly form an alloy protective layer on the surface of pure Zn anode.[67] Zhang *et al.*[50] successfully prepared a novel sandwich-structured Ni-Zn alloy by electrodeposition and two-step annealing method, allowing the symmetric cell to operate stably for 1900 hours at 0.5 mA cm^{-2} (Fig. 2c).

2.2. Zn ions intercalated anode

Just as its name implies, Zn ions intercalated anode would be a kind of anode based on the insertion/extraction mechanism. Drawing inspiration from the electrochemical behavior of Zn^{2+} intercalation in diverse cathode materials, employing an anode material with an appropriate tunnel structure or larger interlayer spacing is a logical and promising strategy.[36,68,69] At present, Zn^{2+}-intercalation anodes primarily consist of sulfides (Fig. 2d)[51] and molybdenum–vanadium oxides (Fig. 2e).[52] The advancement of these anodes offers valuable insights and strategies for the exploration of novel anode materials in aqueous ZIBs.

The study of zinc anode materials has consistently faced challenges, including the proliferation of zinc dendrites, limited reversibility suffered, and a variety of adverse reactions. A range of tactics have been formulated to tackle these difficulties. This encompasses the structural architecture and interface safeguarding of zinc anodes, both primarily targeting the stabilization of the zinc stripping/plating layer. Eliminating *in situ* dendrites, along with corrosion and passivation, are also efficient methods for extending battery duration. Additionally, scientists have developed appropriate low-voltage Zn^{2+}-intercalated anodes as substitutes for the existing metal zinc anode. Intercalated anodes demonstrate substantial storage for Zn^{2+}, offering superior rate efficiency and cycle steadiness in ZIBs. Even with considerable advancements in high-performance zinc anode research, existing optimization methods fall short in addressing issues like dendrite development and various side reactions. Ongoing goal for research is to achieve extended lifespans, greater capacity, and enhanced coulombic efficiency in the zinc anode.

2.3. Summary of this chapter

The anode design in zinc-ion batteries (ZIBs) is crucial for performance, with materials classified into (1) Zn stripping/plating anodes (*e.g.*, metallic Zn) and (2) Zn^{2+}-intercalation anodes. Metallic Zn offers high capacity but suffers from dendrite growth, corrosion, and passivation, which degrade efficiency and safety. To address these issues, three key strategies have been developed: (1) surface modification (*e.g.*, MOFs, carbon coatings) to homogenize Zn deposition and suppress side reactions; (2) structural design (*e.g.*, 3D porous scaffolds) to reduce local current density and dendrite formation; and (3) Zn alloying (*e.g.*, Zn–Al, Ni–Zn) to enhance cycling stability. Alternatively, Zn^{2+}-intercalation anodes (*e.g.*, sulfides, Mo–V oxides) provide dendrite-free operation with improved rate capability. Despite progress, challenges remain in achieving long-term stability and high capacity, driving

ongoing research into advanced materials and interfacial engineering for next-generation ZIBs.

3. Cathode materials of ZIBs

Selecting an appropriate cathode material is vital as it significantly influences the operating voltage and capacity of ZIBs. An ideal cathode material should fulfill these criteria: Selecting an appropriate cathode material is crucial, as it significantly affects the operating voltage and capacity of ZIBs. An ideal cathode material should meet several key criteria to ensure optimal performance, including high electrochemical stability, high electrode potential, favorable energy density, abundant Zn^{2+} storage sites, and compatibility with the aqueous electrolyte system commonly used in ZIBs.[8,70,71]

At present, the choices of cathode materials for ZIBs primarily concentrates on manganese/vanadium-based oxides, Prussian blue analogues, spinel-structured oxides, organic materials, Chevrel phase compounds, layered sulfides, polyanionic compounds, and a few others. In this section, the selection of cathode materials according to the type would be elaborated.

3.1. Manganese-based oxides

The fascination with manganese-based oxides in the realm of electrochemical domain stems from their abundant natural presence, affordability, ecological suitability, and notably abundant redox chemical properties (Fig. 3a).[72] Owing to the unique electronic structure of manganese, manganese oxides with several valence states exhibit diverse crystal formations. Taking MnO_2 for a case study, it possesses an abundant crystalline formation, including α-, β-, γ-, δ-, λ-, and R-types (Fig. 3b).[73]

The orange and blue octahedra surround spin up and down Mn atoms, respectively. The red atoms represent oxygen atom.[73] In essence, basic coordination polyhedron is an octahedral unit composed of six oxygen atoms and one Mn atom. Various types of polymorphs can be established by connecting MnO_6 octahedral units through edges and/or corners, which can be further divided into three categories:

(1) Tunnel type. Tunnel MnO_2 polymorphs exist in several forms, including α-, β-, and γ-MnO_2, which are distinguished primarily by the size and structure of their tunnels. These tunnel variations directly influence the electrochemical properties of the material, such as ion diffusion pathways, structural stability, and overall performance as a cathode in ZIBs. The different tunnel sizes create distinct ionic conductivity and capacity characteristics, making each polymorph suitable for specific applications within energy storage technologies.[73]

(2) Layered type. Layered MnO_2 structures are formed by arranging MnO_6 octahedral units into layers through edge-sharing connections. The interlayer space can accommodate water molecules or a variety of cations, such as Na^+, K^+, or Zn^{2+}, which contribute to an increase in the interlayer distance and enhance ion diffusion capabilities. This ability to host different cations plays a crucial role in improving the electrochemical performance of layered MnO_2, particularly in applications like ZIBs. A typical example of this layered structure is δ-MnO_2, which exhibits excellent ion-exchange properties and structural flexibility, making it a promising candidate for energy storage systems. The intercalation of cations within δ-MnO_2 can facilitate reversible redox reactions, thereby enhancing both capacity and cycling stability in battery applications.

(3) Spinel-type structure. The spinel-type structure (λ-MnO_2) represents a unique polymorph of MnO_2 in which manganese ions occupy specific crystallographic sites: Mn^{2+} are typically located in tetrahedral sites, while Mn^{3+} occupy octahedral positions. Unlike the tunnel or layered structures of other MnO_2 polymorphs, the spinel-type λ-MnO_2 features a densely packed three-dimensional network, which

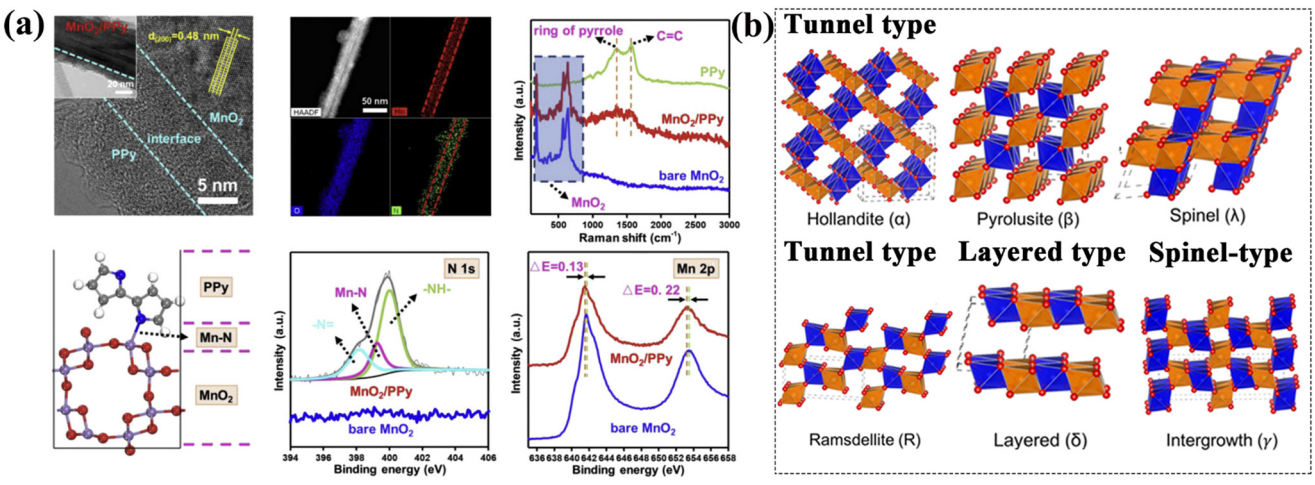

Fig. 3 (a) Characterizations of MnO_2/polypyrrole electrode for ZIBs, including TEM (inset), HRTEM, Raman, and XPS. Reproduced with permission from ref. 72. Copyright 2020. Elsevier. (b) Different MnO_2 polymorphs. Reproduced with permission from ref. 73. Copyright 2018, American Chemical Society.

contributes to its high structural stability and favorable electrochemical properties. This dense packing allows for a more efficient pathway for electron transport, although it also presents challenges in terms of ion diffusion compared to tunnel or layered variants.

All the aforementioned MnO_2 polymorphs, including tunnel-type, layered-type, and spinel-type, can serve as cathode materials for ZIBs. MnO_2 in different polymorphism adhere to distinct electrochemical reaction processes across diverse electrochemical systems,[74] which would be encapsulated in Table 1.

Each polymorph offers distinct advantages, such as enhanced ion diffusion, structural stability, or higher capacity retention, depending on the nature of the MnO_2 structure. However, despite their potential, there remain critical challenges that need to be addressed. Issues such as limited cycle stability, dissolution of Mn in the electrolyte, and relatively sluggish ion diffusion in certain structures must be overcome to optimize their performance in practical ZIB applications. Further research is required to improve the durability, efficiency, and scalability of these MnO_2-based cathode materials for the next generation of sustainable energy storage solutions.

(1) Mn dissolution. First of all, manganese-based oxide cathodes may experience rapid capacity fading owing to the manganese dissolution and structural deterioration. The consensus at the present stage is that the primary cause of this dissolution is a disproportionation reaction, in which Mn^{3+} changes into Mn^{2+} and Mn^{4+} at the junction of the manganese-based cathode and the electrolyte throughout the cycling process.[82] Besides, dissolution from manganese-based oxides is influenced by factors including Jahn–Teller structural distortion, non-fluctuating phase transitions, and recurrent structural alterations. To address this issue, it is anticipated that introducing Mn salt with substantial anion clusters into the electrolyte beforehand will obstruct the dissolution.[72,82] The α-MnO_2 cathode demonstrates remarkable reversibility and stability in a $ZnSO_4$ aqueous electrolyte with a $MnSO_4$ additive, effectively suppressing the dissolution of Mn^{2+} into the electrolyte.[83] At the same time, related reports suggest widespread use of surface coatings to prevent manganese disintegration,[84,85] suggesting an ideal solution for the aforementioned problems. Zhou and his co-workers demonstrated a precisely tailored Ti(III)-concentrated spinel-like interface in a layered manganese-based oxide, effectively preventing Mn dissolution and simultaneously improving the efficiency of electron and ion conductivity.[85]

(2) Sluggish ion diffusion kinetics. As for ZIBs, Zn^{2+} would enjoy the elevated charge density, suffering strong electrostatic bonds with H_2O molecules in aqueous electrolytes, which takes shape a solvent configuration of $Zn–(H_2O)_6^{2+}$, along with a larger molecular dimension up to 5.5 Å, despite the radius of Zn^{2+} being merely 0.76 Å.[86] Prior to insertion Zn^{2+} into manganese-based oxide, considerable energy is needed for the desolvation process to liberate Zn^{2+} from the compact H_2O solvation sheath. Compared with other monovalent charge carries such as Li^+ or Na^+, divalent Zn^{2+} triggers intense

Table 1 Zinc-ion storage mechanism of MnO_2 in different crystallographic structures

Materials	Reaction path			Ref.
α-MnO_2	1	Anode	$Zn \leftrightarrow Zn^{2+} + 2e^-$	75
		Cathode	$Zn^2 + 2e^- + 2MnO_2 \leftrightarrow ZnMn_2O_4$	
	2	Anode	$Zn \leftrightarrow Zn^{2+} + 2e^-$	76
		Cathode	$MnO_2 + H^+ + e^- \leftrightarrow MnOOH$	
			$MnOOH + Zn^{2+} + e^- \rightarrow ZnMn_2O_4$	
	3	Anode	$Zn \leftrightarrow Zn^{2+} + 2e^-$	77
		Cathode	$MnO_2 + xZn^{2+} + 2xe^- \rightarrow Zn_xMnO_2$	
			$MnO_2 + H^+ + e^- \rightarrow MnOOH$	
			$4Zn^{2+} + 6OH^- + SO_4^{2-} + 5H_2O \rightarrow ZnSO_4{\cdot}3Zn(OH)_2{\cdot}5H_2O$	
			$2MnO_2 + 2H^+ + 2e^- \rightarrow Mn_2O_3 + H_2O$	
			$3(ZnSO_4{\cdot}3Zn(OH)_2{\cdot}5H_2O) + 3Mn^{2+} + 8e^- \rightarrow ZnMn_3O_7{\cdot}3H_2O + 8Zn^{2+} + 18OH^- + 3ZnSO_4 + 12H_2O$	
			$Zn_xMnO_2 + (0.5 - x)Zn^{2+} + (1 - 2x)e^- \rightarrow 0.5ZnMn_2O_4$	
			$Zn_2Mn_3O_8 + Mn^{2+} \rightarrow 2ZnMn_2O_4$	
β-MnO_2	1	Anode	$Zn \leftrightarrow Zn^{2+} + 2e^-$	78
		Cathode	$MnO_2 + H^+ + e^- \leftrightarrow MnOOH$	
			$MnOOH + 3H^+ + e^- \leftrightarrow Mn^{2+} + H_2O$	
			$4Zn^{2+} + SO_4^{2-} + 8H_2O \leftrightarrow Zn_4SO_4(OH)_6{\cdot}5H_2O + 6H^+$	
γ-MnO_2	1	Anode	$Zn \leftrightarrow Zn^{2+} + 2e^-$	79
		Cathode	$2\gamma\text{-}MnO_2 + Zn^{2+} + 2e^- \leftrightarrow$ spinel $ZnMn_2O_4$	
			Spinel $ZnMn_2O_4 + (2x - 1)Zn^{2+} + (2x - 1)e^- \leftrightarrow 2\gamma\text{-}Zn_xMnO_2$ tunnel-type	
			$\gamma\text{-}Zn_xMnO_2$ tunnel-type ↔ L-Zn_xMnO_2 (layered-type)	
δ-MnO_2	1	Anode	$Zn \leftrightarrow Zn^{2+} + 2e^-$	80
		Cathode	$Zn + 2MnO_2 \leftrightarrow ZnMn_2O_4$	
			$Zn + MnO_2 \leftrightarrow ZnMnO_2$	
	2	Anode	$(1/2 + x)Zn \leftrightarrow (1/2 + x)Zn^{2+} + (1 + 2x)e^-$	81
		Cathode	$MnO_2 + xZn^{2+} + 2xe^- \leftrightarrow Zn_xMnO_2$ (non-diffusion controlled)	
			$H_2O \leftrightarrow H^+ + OH^-$	
			$MnO_2 + H^+ + e^- \leftrightarrow MnOOH$ (diffusion controlled)	
			$1/2Zn^{2+} + OH^- + 1/6Zn(TFSI)_2 + x/6H_2O \leftrightarrow 1/6Zn(TFSI)_2[Zn(OH)_2]_3{\cdot}xH_2O$	

electrostatic repulsion, resulting in slow solid-state diffusion kinetics in contrast to the monovalent charge carriers.[87] In view of this, manipulating the microstructure of MnO_2 aids in refining the diffusion paths of Zn^{2+}. Guo *et al.* prepared ultrathin δ-MnO_2 nanosheets as cathode for aqueous rechargeable ZIBs, demonstrating a better performance than δ-MnO_2 microspheres.

(3) Poor electrical conductivity. In general, MnO_2 electrodes exhibit low intrinsic electronic conductivity due to the peculiarity of semiconductor, which can be seriously detrimental its electrochemical performance. Aiming for this dilemma, some strategies such as element doping, defect engineering, and conductive material composited can be adopted. Besides MnO_2, different stoichiometric proportions of manganese oxide, like Mn_2O_3 (ref. 88) or Mn_3O_4,[89] can be suitable for use in cathode of ZIBs as well.

3.2. Vanadium-based compounds

The diverse valence states of vanadium, ranging from +2 to +5, have facilitated the exploration of a wide range of chemical compositions and crystal structures. Various vanadium-based compounds, including vanadium oxides,[90] vanadium phosphates,[91] vanadates,[92] vanadium sulfides,[93] and vanadium nitrides,[94] have been investigated as potential cathode materials for ZIBs. In this review, we provide a comprehensive overview of recent advancements in vanadium-based electrode materials for aqueous ZIBs, highlighting their structural characteristics, electrochemical performance, and the challenges that remain for their practical application.

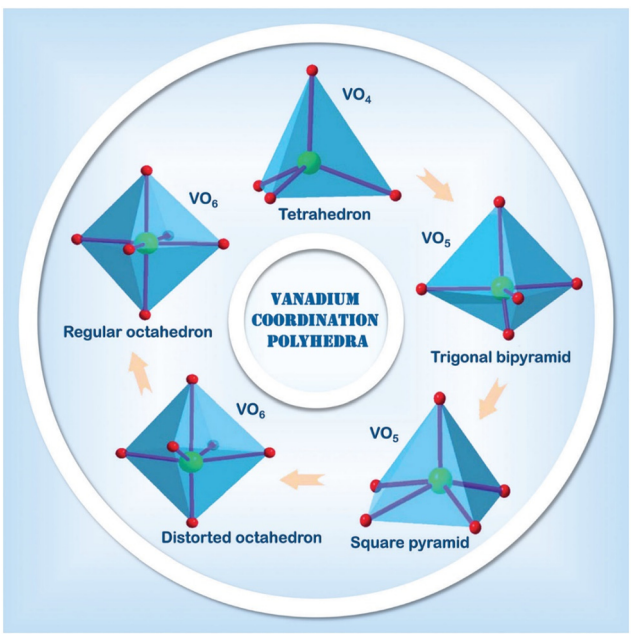

Fig. 4 Various vanadium coordination polyhedrons (red O atoms, green V atoms, and pink V–O bonds). Reproduced with permission from ref. 97. Copyright 2023. WILEY-VCH Verlag GmbH & Co. KGaA, Weinheim.

Table 2 Zinc-ion storage mechanism of different vanadium-based oxides

Materials	Reaction path		Ref.
VO_2	Anode	$Zn \leftrightarrow Zn^{2+} + 2e^-$	97
	Cathode	$H^+ + e^- + VO^{2+} \leftrightarrow HVO_2$	
V_2O_3	Anode	$Zn^{2+} + 2e^- \leftrightarrow Zn$	97
	Cathode	$V_2O_3 + xZn^{2+} + nH_2O + 2xe^- \leftrightarrow Zn_xV_2O_3{\cdot}nH_2O$	
V_2O_5	Anode	$Zn \leftrightarrow Zn^{2+} + 2e^-$	90
	Cathode	$xZn^{2+} + V_2O_5 + 2xe^- \leftrightarrow Zn_xV_2O_5$	

3.2.1. Vanadium-based oxides. Fundamental V–O coordination polyhedral are constructed into various structures of vanadium oxides. Interestingly, the vanadium atom and the oxygen atom have multiple coordination forms, varying from tetrahedron through square pyramid and trigonal bipyramid to distorted and regular octahedra (Fig. 4).[95–97] The ongoing alterations in complex polyhedral and oxidation state of vanadium can be effectively modified to host Zn^{2+}, resulting in effective electrochemical performance. Fascinatingly, various vanadium oxides demonstrate distinct methods of Zn^{2+} storage, attributed to their unique crystal configurations, which can be further summarized in Table 2.[97]

3.2.2. Vanadyl phosphates. Vanadyl phosphate plays a crucial role in the vanadium-based compounds cathode family, which can boost the redox potential by the inductive effect of the polyanion PO_4^{3-}.[98,99] Besides, the intense polarization of the electrons of O^{2-} into strong covalent bonding within the polyanion can reduce the covalent bond between vanadium and oxygen, lowering its redox energy.[98,100] As for a basic example, $VOPO_4$ can be characterized by a corner-sharing VO_6 octahedron linked to the PO_4 tetrahedron, serving as a typical polyanion cathode with associated two-dimensional diffusion channels (Fig. 5a).[101] Besides, other types of vanadyl phosphates, including $VOPO_4{\cdot}2H_2O$ (ref. 102) and $KVOPO_4$,[103] can be used as excellent cathode for ZIBs (Fig. 5b and c).

3.2.3. Vanadium-based NASICON-type phosphates. The NASICON-type phosphates, featuring a sodium superionic conductor configuration, possess an extensively covalent three-dimensional host structure with ample clearance, facilitating ion diffusion efficiently,[98] which has been demonstrated in LIBs[106] and sodium-ion batteries (SIBs).[106] However, radius of Zn^{2+} (0.74 Å) can be smaller than that of Na^+ (1.02 Å),[107,108] which may pave the way for applying NASICON-type phosphates as the cathode material of ZIBs. Li and his co-workers[109] firstly developed NASICON structured $Na_3V_2(PO_4)_3$ for aqueous ZIBs, delivering a reversible capacity of 97 mA h g^{-1} at 0.5 C and retains 74% capacity after 100 cycles. Furthermore, the energy density and redox potential of NASICON-type phosphate structures surpass those of similar vanadium oxides, attributed to the potent inducible influence of PO^{3-} polyanion and the robust P–O bond.[97]

3.2.4. Vanadates. Typically, a variety of vanadates can be synthesized by layering vanadate oxides with diverse cation types. The crystal structure and electrochemical

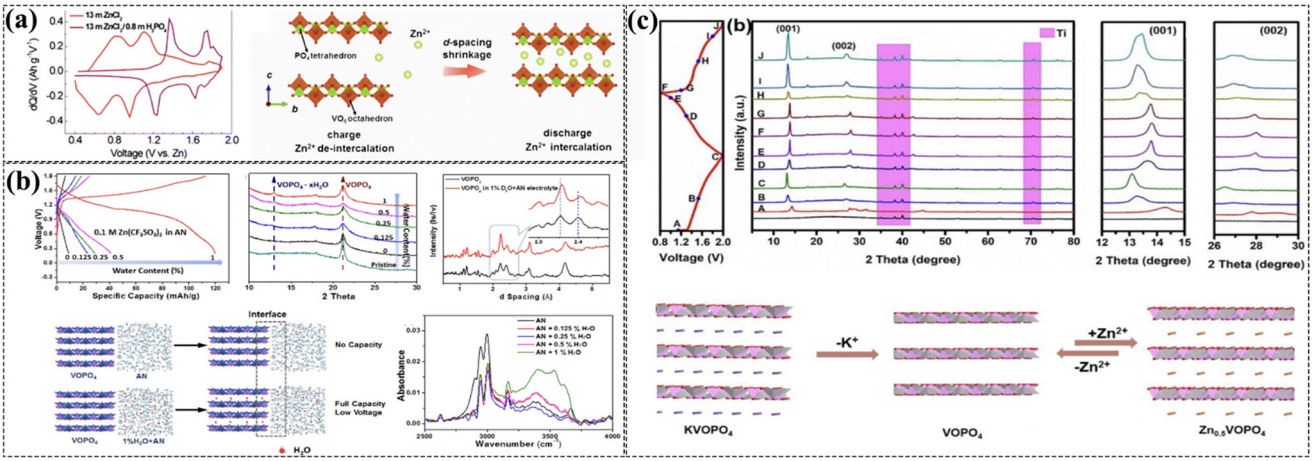

Fig. 5 (a) Schematic illustration of the Zn^{2+} (de)intercalation mechanism in the bilayer $VOPO_4$ nanosheets. Reproduced with permission from ref. 104. Copyright 2021. WILEY-VCH Verlag GmbH & Co. KGaA, Weinheim. (b) $VOPO_4{\cdot}2H_2O$ for ZIBs. Reproduced with permission from ref. 102. Copyright 2018, WILEY-VCH Verlag GmbH & Co. KGaA, Weinheim. (c) $KVOPO_4$ electrodes for ZIBs. Reproduced with permission from ref. 105. Copyright 2021, Elsevier Ltd.

characteristics of vanadate are primarily influenced by three factors: the variety of metal ions, changes in M/V ratios (with M representing additional metal ions), and fluctuations in vanadium valance.[110] Within the particular experimental framework, the aforementioned parameters should be meticulously modified to suit the requirements of various electrochemical systems. To be specific, although the advantages like the pillar-effect could be granted to expand the layer-spacing available for incorporating more Zn^{2+}, ions intercalated within the vanadates formations can be ejected from the crystal structure and subsequently dissolved in the electrolyte, resulting in rapid degradation of capacity.[9,111,112]

3.2.5. Other vanadium-based compounds. The potential of vanadium sulfides, including VS_2,[113] VS_4 (ref. 114) and V_3S_4 (ref. 115) as well as vanadium nitride (VN),[116] as cathode materials for ZIBs, is also under active investigation. These vanadium-based compounds offer distinct electrochemical properties that make them promising candidates for high-performance energy storage applications. The layered structure of VS_2 (Fig. 6a), for example, allows for efficient zinc-ion intercalation, while the unique bonding environment in VS_4 (Fig. 6b)[114] and V_3S_4 (Fig. 6c)[115] contributes to enhanced electronic conductivity and structural stability. Similarly, vanadium nitride (VN)[116] (Fig. 6d) demonstrates excellent electrical conductivity and robust cycling performance, making it an attractive material for ZIB cathodes. This review aims to provide a detailed analysis of the latest research progress on vanadium sulfides and nitrides, emphasizing their structural characteristics, electrochemical behavior, and the challenges that need to be addressed to realize their full potential in practical ZIBs application.

3.3. Prussian blue analogues

Extensive research has been conducted on Prussian blue analogues (PBAs) as hosts for metal-ion batteries, characterized by their adoption of three-dimensional open-structure configurations, numerous redox-active sites, and significant structural steadiness.[117,118] The ideal PBA is indicated by the equation $A_2M_AM_B(CN)_6$ (Fig. 7a), where A denotes as Li^+, Na^+, K^+, zeolite water, and M_A symbolizes Fe, Ni, Mn, V, Mo, Cu, Co, Zn, and M_B signifies Fe, Co, Cr, Ru. Owing to its robustness in aqueous solutions, ferricyanide stands as the main raw material for synthesis, resulting in a majority of M_B sites within this structure being filled by Fe atmos. PBA represents a kind of metallic compound with a body-centered cubic configuration, where nitrogen and carbon atoms from C≡N ligand link with M_B and M_A atoms to create open ion channels and expansive interstitial gaps.[119] Zhang *et al.*[120] demonstrated the feasibility for zinc hexacyanoferrate ($Zn_3[Fe(CN)_6]_2$, ZnHCF) as cathode for aqueous ZIBs, showing high operating voltage (Fig. 7b). In PBAs, the M_B site exemplifies the redox active site in this configuration. That is to say, replacing a distinct transition metal M_A affects the reaction potential and the ability of PBAs. Different or the same metal atoms inhabit the M_A and M_B locations, leading to unique combination and reaction potentials.[121,122] The elements Fe, Mn, Co, and V exhibit electrochemical activity within the stable range of the organic electrolyte and aqueous system in PBAs. A double-electron redox reaction may take place when these metal ions fill the M_A site.

Based on the redox sites involved in the reaction, PBA-based cathode materials can be divided into two categories: a single redox pair and double redox pair. As for a single redox pair PBA-based cathode, it shows a pair of anodic/cathodic react ion peaks, while two pairs presented for the cathode of double redox pair. Advances in *in situ* characterization techniques have helped researchers better understand the presence of double REDOX pairs in electrochemical mechanisms. Yang *et al.*[123] presents innovative insights into the electrochemical mechanisms of

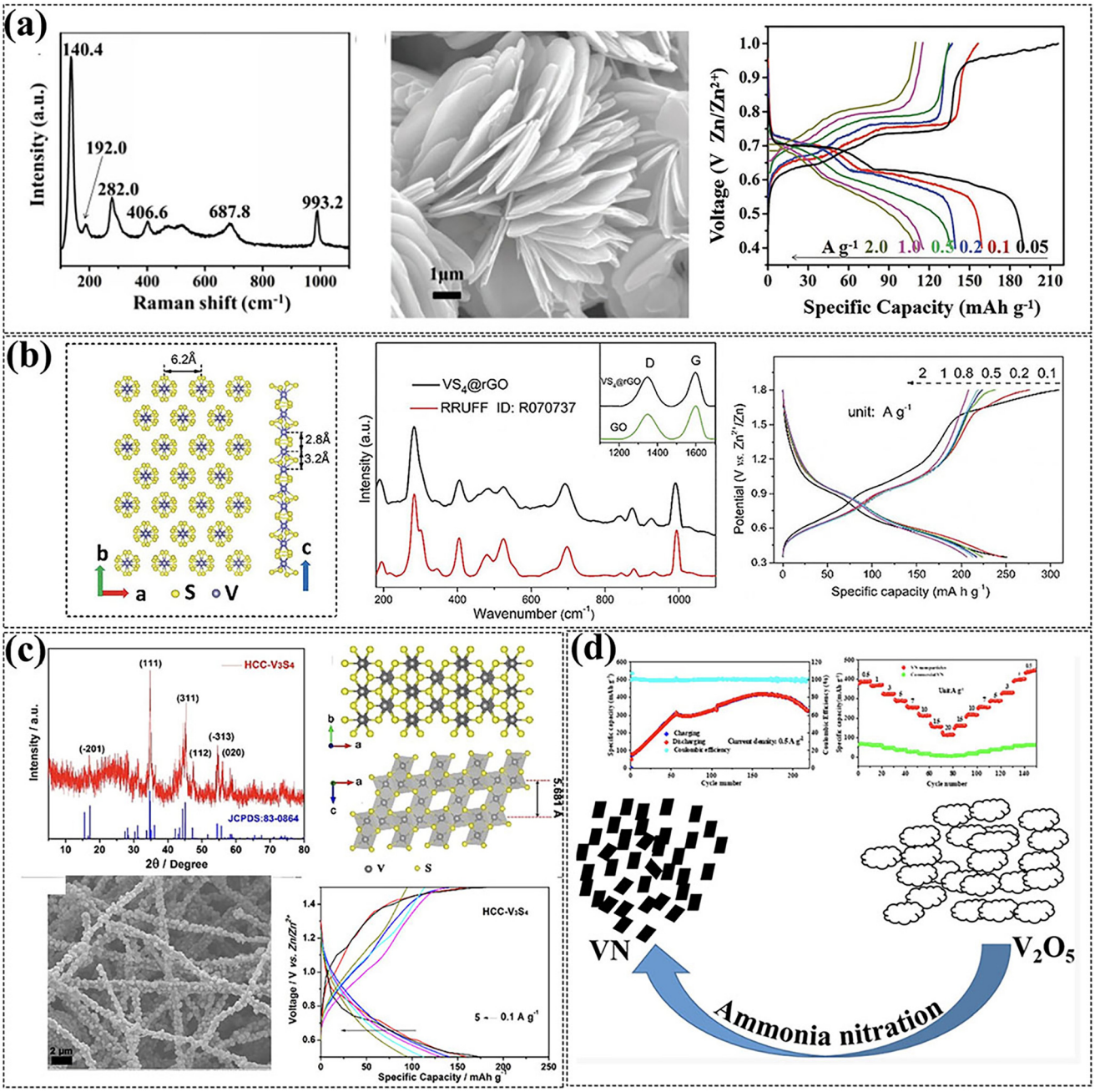

Fig. 6 (a) VS_2 cathodes for ZIBs. Reproduced with permission from ref. 113. Copyright 2017, WILEY-VCH Verlag GmbH & Co. KGaA, Weinheim. (b) VS_4 cathodes for ZIBs. Reproduced with permission from ref. 114. Copyright 2018, Royal Society of Chemistry. (c) V_3S_4 cathodes for ZIBs. Reproduced with permission from ref. 115. Copyright 2019, American Chemical Society. (d) VN cathodes for ZIBs. Reproduced with permission from ref. 116. Copyright 2021, American Chemical Society.

vanadium hexacyanoferrate (VOHCF) as a cathode material. As the charge impelling, the strength of the V═O between 864–921 cm^{-1} steadily reduces, suggesting a gradual process of ion insertion. When discharged, the intensity for V═O peak gradually intensifies, indicating the possibility of reversible ion intercalation and de-intercalation into VOHCF. Besides, the $[Fe(CN)_6]^{4-}$ group gradually shifts to higher wavenumbers, followed by a reverse migration that corresponds to Fe^{2+} to Fe^{3+}, thereby demonstrating the pivotal role of $[Fe(CN)_6]^{4-}$ as an additional REDOX active site.

PBAs are emerging as highly promising cathode for ZIBs due to their unique combination of high theoretical capacity, excellent cycling stability, and rapid ion diffusion kinetics enabled by their open-framework structures.[124] These materials offer significant advantages, including cost-effectiveness, environmental benignity, and compatibility with aqueous electrolytes, which collectively support their

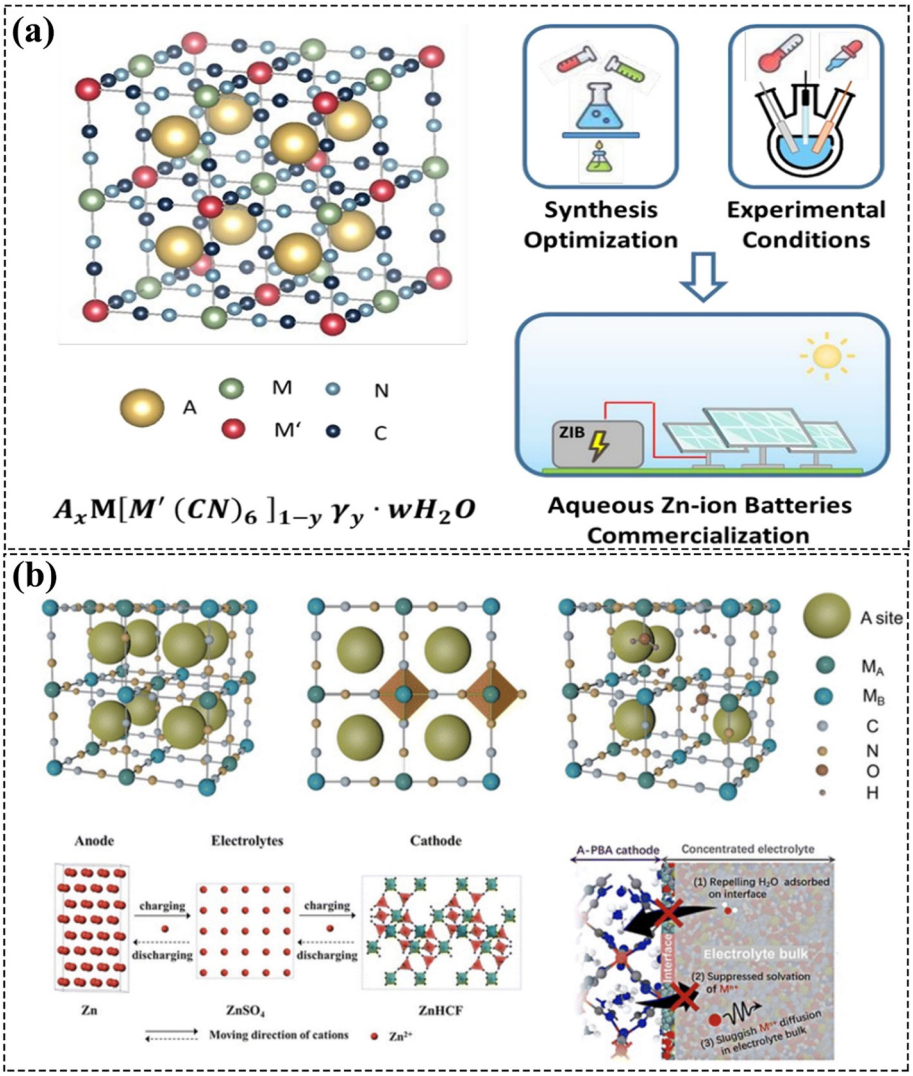

Fig. 7 (a) Schematic representation of the crystal structure of the class of materials belonging to the PBAs. Reproduced with permission from ref. 117. Copyright 2020, Elsevier Ltd. (b) Prussian blue ideal framework and its coordination form. Reproduced with permission from ref. 119. Copyright 2024, Royal Society of Chemistry.

potential for ideal cathode. However, PBAs also face challenges such as relatively low electrical conductivity, which can impede rate performance, and potential structural degradation in highly acidic or alkaline electrolytes over prolonged cycling. Despite these limitations, ongoing research efforts aimed at enhancing conductivity through composite formulations and optimizing structural stability are paving the way for PBAs to overcome these hurdles, thereby positioning them as a viable and sustainable solution for next-generation ZIBs.

3.4. Organic materials

The appeal of organic compounds, including small molecules and polymers, as electrode materials for aqueous ZIBs lies in their eco-friendly nature, structural versatility, cost-effectiveness, and tunable electrochemical properties.[125,126] Unlike conventional inorganic cathodes, organic materials are inherently sustainable, composed of abundant light elements such as carbon (C), hydrogen (H), oxygen (O), nitrogen (N), and sulfur (S), eliminating reliance on scarce or toxic heavy metals (*e.g.*, Co, Ni). These materials can be synthesized through scalable artificial routes or derived from renewable biomass resources, aligning with green chemistry principles. Critically, their molecular and polymeric frameworks allow for precise customization of physical properties (*e.g.*, solubility, porosity, and electronic conductivity) and electrochemical performance (*e.g.*, redox potentials, ion-binding affinity) *via* functional group engineering or conjugation extension.[127] Furthermore, the redox mechanisms in organic electrodes differ fundamentally from inorganic counterparts: instead of Zn^{2+} intercalation/deintercalation, which induces structural strain and phase transitions, organic materials undergo reversible bond reorganization (*e.g.*, enolization, proton-coupled electron transfer) during charge/discharge, enabling

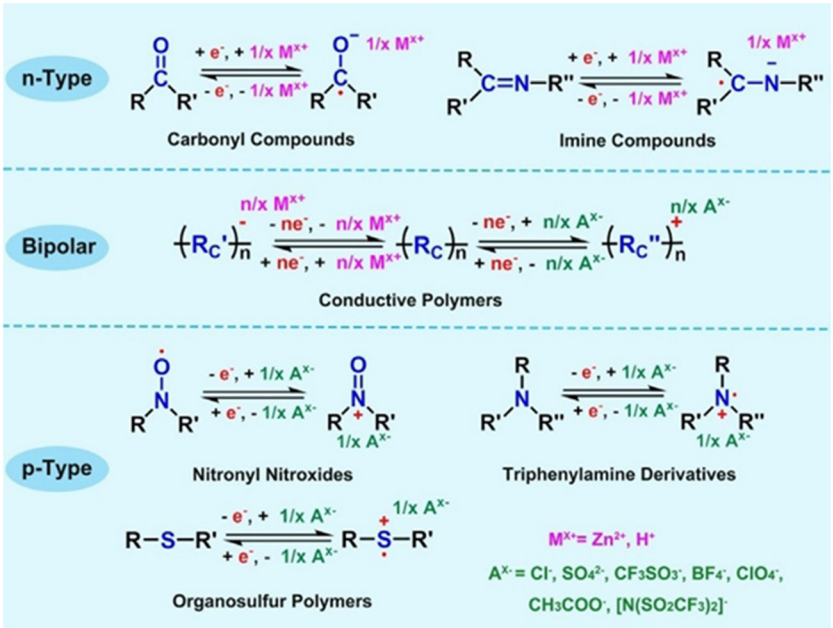

Fig. 8 The energy storage mechanisms of different types of organic electrode materials in aqueous ZIBs. Reproduced with permission from ref. 126. Copyright 2017, WILEY-VCH Verlag GmbH & Co. KGaA, Weinheim.

smoother ion accommodation and reduced mechanical degradation.[126]

Organic electrode materials are classified into three categories based on their redox-active functional groups and charge-compensation mechanisms during cycling (Fig. 8):

(1) n-Type organic materials. n-Type organic compounds, such as quinones, imides, and carbonyl-based polymers, operate *via* anion-forming reduction reactions.[128] During discharge, their redox-active centers (*e.g.*, carbonyl groups, C═O) undergo reduction, generating negatively charged enolate or radical anions. These anions stabilize through coordination with cations (*e.g.*, Zn^{2+}, H^+) from the electrolyte, enabling reversible Zn^{2+} storage. For example, in a quinone-based cathode, the reduction of C═O to C–O^- during discharge attracts Zn^{2+} ions, forming a Zn–organic complex. Upon charging, the process reverses, releasing Zn^{2+} back into the electrolyte. A key advantage of n-type materials is their high theoretical capacity (often >300 mA h g^{-1}) due to multi-electron redox reactions. However, challenges include solubility in aqueous electrolytes (leading to capacity fade) and sluggish kinetics caused by strong electrostatic interactions between Zn^{2+} and the organic matrix. Strategies to mitigate these issues involve polymerization, cross-linking, or hybridization with conductive carbon networks to enhance stability and charge transfer.

(2) p-Type organic materials. p-Type organic materials, such as conductive polymers (*e.g.*, polyaniline, polythiophene) and radical-containing compounds, function through oxidation-driven cation storage. During charging, these materials lose electrons from their conjugated backbones or radical sites, forming positively charged species (*e.g.*, polaron or bipolar on states in polymers). To maintain charge neutrality, anions (*e.g.*, SO_4^{2-}, $CF_3SO_3^-$) from the electrolyte migrate into the cathode and bind to the oxidized sites. During discharge, the reverse process releases anions while electrons are transferred back to the organic framework. p-Type materials often exhibit high operating voltages due to their oxidative redox potentials, but their capacities are typically lower than n-type counterparts. A major limitation is parasitic side reactions, such as over-oxidation of the polymer backbone in acidic electrolytes, which degrades cyclability. Recent advances focus on designing stable redox-active units (*e.g.*, phenazine, triazine) and optimizing electrolyte pH to suppress irreversible oxidation.[129]

(3) Bipolar-type organic materials. Bipolar-type organic materials integrate both n-type and p-type redox-active moieties within a single structure, enabling dual-ion storage mechanisms. For instance, a conjugated polymer with alternating electron-deficient (p-type) and electron-rich (n-type) units can undergo sequential oxidation and reduction during cycling. During charging, the p-type segments oxidize and host anions, while the n-type segments reduce and bind cations (*e.g.*, Zn^{2+}). This dual-mode operation allows bipolar materials to achieve higher energy densities by leveraging both cation and anion charge compensation. Examples include anthraquinone-based covalent organic frameworks (COFs) and donor–acceptor polymers. However, the complexity of balancing redox potentials and kinetics between the two mechanisms often leads to voltage hysteresis or incomplete reversibility. Tailoring molecular symmetry, π-conjugation length, and ion transport pathways through supramolecular design is critical to unlocking their full potential.

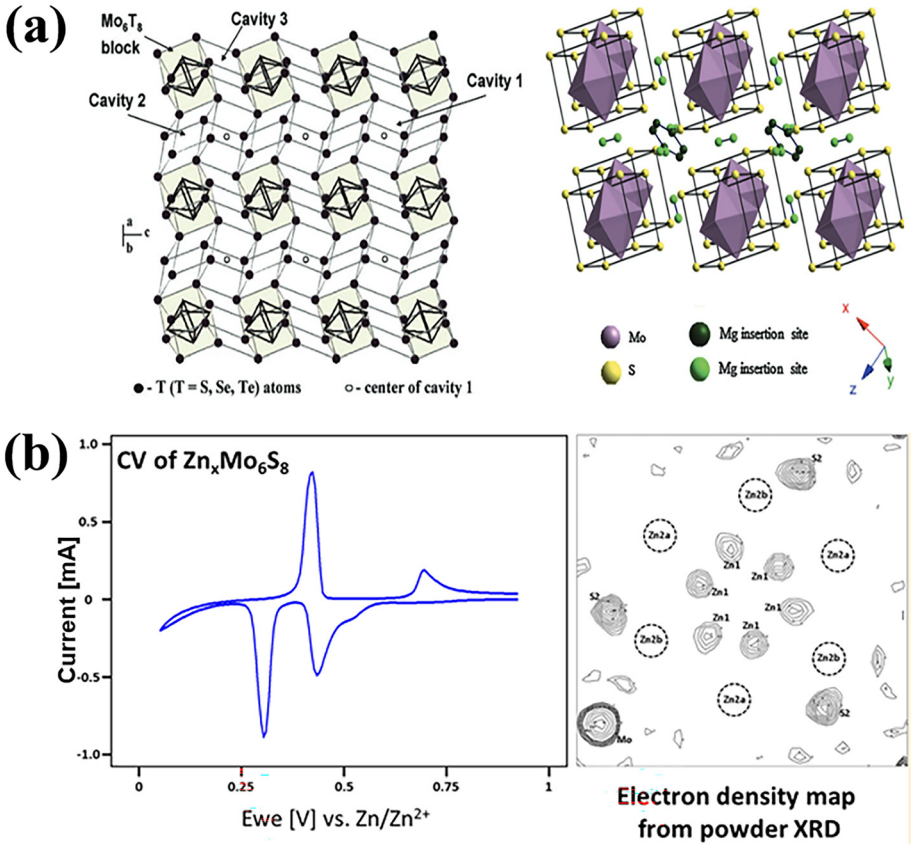

Fig. 9 (a) Different schematic presentation of graphic structure of Mo_6T_8 and Mo_6S_8 and typical discharge–charge profiles of Mo_6Se_8 and Mo_6S_8 electrode. Reproduced with permission from ref. 130. Copyright 2017, WILEY-VCH Verlag GmbH & Co. KGaA, Weinheim. (b) $Zn_xMo_6S_8$ cathode for ZIBs. Reproduced with permission from ref. 136. Copyright 2016, American Chemical Society.

While organic electrodes offer unique advantages for ZIBs, practical deployment requires addressing intrinsic limitations. Their low electronic conductivity often necessitates composite architectures with conductive additives (*e.g.*, carbon nanotubes, graphene). Solubility in aqueous electrolytes remains a persistent issue, particularly for small-molecule organics, driving research into covalent immobilization strategies or gel-based electrolytes. Furthermore, the redox mechanisms of many organic materials involve H^+ co-insertion, which complicates Zn^{2+} storage quantification and may accelerate hydrogen evolution at the anode. Future work should prioritize in operando characterization (*e.g.*, X-ray diffraction, Raman spectroscopy) to decouple Zn^{2+}/H^+ contributions and machine learning-guided molecular design to optimize ion selectivity. By synergizing molecular engineering with electrolyte innovation, organic materials could emerge as high-performance, sustainable cathodes for next-generation ZIBs.

3.5. Chevrel phase compounds

Chevrel-phase materials (with the chemical formula Mo_6T_8, where T = S, Se, or their composites) have attracted increasing attention since their discovery in the 1970s due to their unique rigid open-framework structure and excellent ion-insertion capability, making them a research hotspot for multivalent-ion batteries (such as Mg^{2+} and Zn^{2+}).[130] In terms of crystal structure, Chevrel phase Mo_6T_8 with a three-dimensional array of Mo_6T_8 units in which each Mo_6T_8 unit is composed of the octahedral cluster of molybdenum atoms inside the anion cube to form tri-directional channels for metal cations.[131,132] As can be seen in Fig. 9a, there are three different cation locations for Mo_6T_8 (cavities 1, 2 and 3). Cavity 1 is the site far away from Mo atom and share corner with the Mo_6T_8 cube. Cavity 2 and 3 share the edges and faces with Mo_6T_8, respectively. Only the cavities 1 and 2 can be filled by metal cation when cavity 3 is blocked by a strong repulsion of the Mo atoms. Metal cations in cavities 1 or 2 are primarily positioned based on size of M, with M cations of greater atomic size typically situated at the cavity's center. Taking Mg^{2+} as a typical example (Fig. 9b), it insertion into Mo_6T_8 (*i.e.*, T = S) firstly occupies the inner six sites in cavity 1 with an inner ring and the cation occupies in cavity 2 with another six sites with an outer ring. The potential energy of the cation site in cavity 1 is less compared to that in insertion cavity 2. Research has been conducted on various monovalent (like Li, Na) and multi-valent cation (such as Zn, Mg, Al) intercalation-type batteries, grounded in the Chevrel phase's crystal structure.

In recent years, with the rise of aqueous ZIBs, Chevrel-phase materials have been considered as a highly promising cathode material system for ZIBs due to their efficient and reversible storage characteristics for Zn^{2+}. More importantly, the working voltage range of Chevrel-phase materials (0.4–1.2 V *vs.* Zn^{2+}/Zn) highly match the stability window of aqueous electrolytes, avoiding hydrogen-evolution and oxygen-evolution side reactions. Moreover, their intrinsic oxidation-resistance (Mo–S bond energy > 300 kJ mol^{-1}) ensures chemical stability at high temperatures, meeting the stringent safety requirements of ZIBs.[51,133–135] Hong's research team[136] achieved the reversible insertion/extraction of Zn^{2+} in Mo_6S_8 through electrochemical methods, demonstrating the feasibility of Chevrel-phase materials in aqueous ZIBs.

The Chevrel phase garners more interest as a potential electrode for ZIBs due to its distinctive open crystal formation and robust electrochemical behavior.[130] Yet, currently, the synthesis conditions for Chevrel phase remain somewhat stringent relative to other cathode materials, and the challenge of optimizing the preparation conditions deserves a consideration in the future, the employment of synthesis methods such as Joule heating or microwave-assisted strategy may be the remedies.[135]

3.6. MXenes

Two-dimensional transition metal carbides, nitrides and carbonitrides, also termed as MXenes, are recognized for their adaptability owing to their high electrical conductivity and rich surface chemistry.[137,138] Like many two-dimensional materials, MXene follows a typical intercalation mechanism when applied directly to the cathode for the ZIBs, offering inherent benefits as a cathode material for ZIBs, not only can it be used directly as an active material to host Zn^{2+}, but also as a stable conductive network to be combined with other materials.[137,139,140] Huang *et al.*[141] delved into the intricate characteristics of different MXene materials containing different halogen groups in the molt salt, it is found that the electrochemical properties of MXene cathodes for ZIBs can be optimized effectively by adjusting the types of terminal groups. Besides, owing to the superior conductivity and hydrophilicity, it's feasible to composite MXene with active material possessing greater theoretical capacity. Using transition metal oxides as a case study, while their conductivity is typically low, but electrochemical performance can be enhanced after composited with MXene. Yan *et al.*[142] prepared an innovative 3D MXene–MnO_2 composite cathode using a gas-phase spray drying technique, encapsulating MnO_2 nanoparticles within the wrinkled MXene nanosheets, resulting in a sturdy, conductive structure resembling a 3D micro-flower, advantageous for quick ion/electron movement and enhanced structural stability. When used as cathode for ZIBs, the $Ti_3C_2T_x$@MnO_2 micro-flowers delivers a high reversible capacity, which can be superior to the pure MnO_2 electrode.

Despite the promising properties of MXenes, several challenges need to be addressed for their practical application in ZIBs. These include ensuring structural stability during long-term cycling, improving ion diffusion kinetics, and addressing the potential toxicity of certain transition metals. Future research should focus on developing advanced synthesis methods to enhance the stability and performance of MXenes, as well as exploring new MXene-based composites to further improve their electrochemical properties. Additionally, the oxidation of MXenes under reactive conditions remains a critical challenge.[143,144] Furthermore, MXene's present production technique primarily involves hydrofluoric acid, where the acid's corrosive nature poses extra safety hazards. Future studies should focus on developing safer and more environmentally friendly methods, which can be the foundation to advance the MXene-based cathode materials for ZIBs.[140,145,146]

In recent years, significant progress has been made in the development of cathode materials for ZIBs. Researchers have explored a wide range of materials, from traditional inorganic compounds to emerging organic and composite materials, each offering unique advantages in terms of voltage, capacity, and cycling stability (Table 3). While some materials have demonstrated high operating voltages and excellent rate

Table 3 Comparison of different cathode materials

Cathode materials	Electrolyte component	Testing voltage (V)	Cycling performance (retention/cycles/rates)	Ref.
α-MnO_2	2 M $ZnSO_4$ + 0.1 M $MnSO_4$	1.0–1.8	92%/5000/1540 mA g^{-1}	83
β-MnO_2	3 M $Zn(CF_3SO_3)_2$ + 0.1 M $Mn(CF_3SO_3)_2$	0.8–1.9	94%/2000/2000 mA g^{-1}	147
V_2O_5	3 M $ZnSO_4$	0.4–1.4	75%/400/100 mA g^{-1}	148
VO_2(B)/RGO	3 M $Zn(CH_3F_3SO_3)$	0.2–1.4	90%/1000/5 A g^{-1}	149
CuHCF	1 M $ZnSO_4$	0.2–1.2	77%/20/20 mA g^{-1}	150
ZnHCF	1 M ZnSO4	0.8–1.9	81%/100/300 mA g^{-1}	120
Quinone(C4Q)	3 M $Zn(CF_3SO_3)_2$	0.2–1.8	87%/1000/500 mA g^{-1}	151
p-Chloranil	1 M $Zn(CF_3SO_3)_2$	0.8–1.4	70%/200/0.2 C	152
VS_2	1 M $ZnSO_4$	0.4–1.4	98%/200/50 mA g^{-1}	113
VS_2-RGO	3 M $Zn(CF_3SO_3)_2$	0.2–1.8	93%/1000/5 A g^{-1}	153
MO_6S_8	1 M $ZnSO_4$	0.25–1.0	95%/150/180 mA g^{-1}	51
V_2CT_x	21 M LiTFSI/1 M $Zn(CF_3SO_3)_2$	0.1–2.0	~100%/2000/10 A g^{-1}	154
VO_2/Ti_3C_2	2 M $Zn(CF_3SO_3)_2$	0.2–1.4	76%/5000/6 A g^{-1}	155

capabilities, others have shown remarkable discharge capacities and long-term cyclability. These advancements highlight the potential for ZIBs to address key challenges in energy storage applications.

However, despite these achievements, several challenges remain. Many cathode materials still suffer from issues such as complex preparation process, harsh storage conditions and so on. Additionally, the complex interplay between material properties and electrolyte interactions limits the practical application of these materials to some extent. Going forward, the architecture of cathode materials for ZIBs must take into account its compatibility with the electrolyte stability window and the theoretical capacity for anode. Moreover, the development of new reaction mechanisms and the exploration of sustainable, cost-effective cathode materials are crucial for the long-term success of ZIBs.

3.7. Summary of this chapter

Cathode materials play a pivotal role in determining the performance of zinc-ion batteries (ZIBs), with ideal candidates requiring high electrochemical stability, favorable energy density, and efficient Zn^{2+} storage. Major cathode categories include (1) manganese-based oxides (α-, β-, γ-, δ-, λ-MnO_2), which offer tunable structures but face challenges like Mn dissolution and sluggish kinetics; (2) vanadium-based compounds (V_2O_5, $VOPO_4$, NASICON-type phosphates), leveraging multiple redox states for high capacity yet hindered by structural instability; (3) Prussian blue analogues

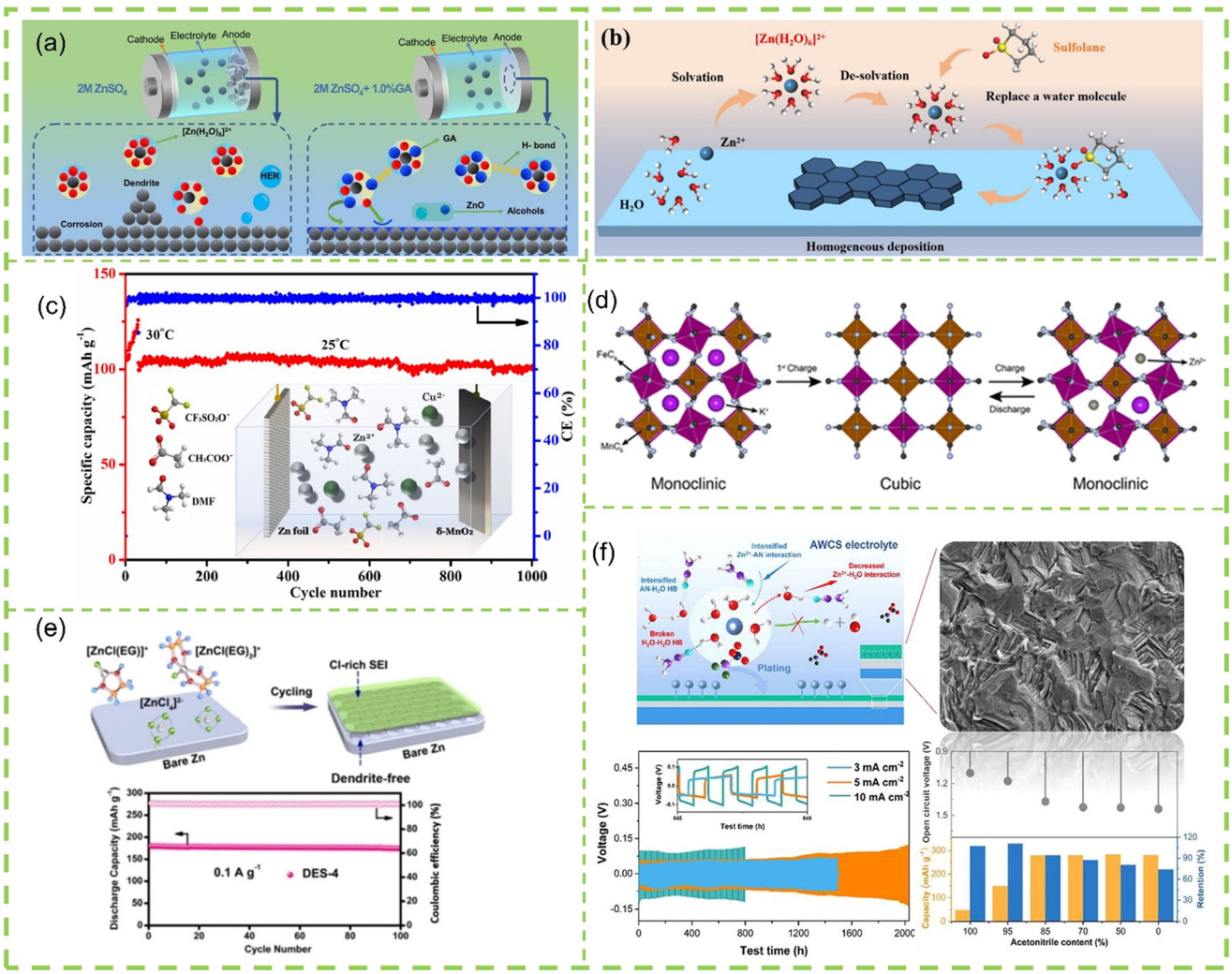

Fig. 10 Liquid electrolytes: (a) a natural multifunctional additive gum arabic into the $ZnSO_4$-based electrolyte. Reproduced with permission from ref. 156. Copyright 2023, Elsevier Ltd. (b) Schematic illustration for Zn deposition cycled in sulfolane/$ZnSO_4$ electrolyte. Reproduced with permission from ref. 157. Copyright 2023, Elsevier Ltd. (c) DMF based nonaqueous electrolyte containing Cu^{2+} as an additive. Reproduced with permission from ref. 158. Copyright, Elsevier Ltd. (d) Schematic diagram of the redox reaction in the $Zn(TFA)_2$-AN-TEP nonaqueous electrolyte. Reproduced with permission from ref. 159. Copyright 2022, American Chemical Society. (e) A new eutectic electrolyte consisting of EG and $ZnCl_2$ for dendrite-free and long-lifespan ZIBs. Reproduced with permission from ref. 160. Copyright 2022, Wiley-VCH Verlag GmbH & Co. KGaA, Weinheim. (f) Acetonitrile is introduced into $Zn(OTf)_2$ electrolyte as co-solvent reproduced with permission from ref. 161. Copyright 2022, Elsevier Ltd.

(PBAs), prized for their open frameworks and dual redox sites but limited by low conductivity; (4) organic materials (n-type, p-type, bipolar), which are sustainable and tunable but suffer from solubility and poor conductivity; (5) Chevrel-phase compounds (Mo_6S_8), enabling reversible Zn^{2+} intercalation with high thermal stability but complex synthesis; and (6) MXenes, valued for conductivity and compositing potential but challenged by oxidation and toxicity. While advancements in structural engineering (*e.g.*, 3D architectures, surface coatings) and electrolyte optimization (*e.g.*, $MnSO_4$ additives) have improved performance, issues like capacity fade, side reactions, and scalability persist. Future research must focus on mechanistic insights, sustainable designs, and compatibility with aqueous electrolytes to realize practical ZIBs.

4. Electrolyte research

The scarcity of resources required for LIBs, flammable and toxic organic electrolytes that are harmful to the environment and safety, and the fact that they cannot be easily recycled limit the further development of LIBs. In contrast, ZIBs are rich in resources, are less prone to thermal runaway at high temperatures or short circuits, and are highly secure, while having a low environmental impact and resources that can be efficiently recovered and recycled. Liquid electrolytes and solid electrolytes are used in different types of ZIBs depending on the application requirements and design decisions of the ZIBs.

4.1. Liquid electrolytes

4.1.1. Aqueous electrolytes. An aqueous electrolyte, employed in ZIBs, is a liquid solution primarily composed of water and certain ionic salts, which facilitate the efficient transport of zinc ions. These aqueous electrolytes encompass both alkaline electrolytes such as LiOH, NaOH, and KOH, as well as neutral or weakly acidic electrolytes, including $Zn(NO_3)_2$, $ZnCl_2$, $ZnSO_4$, $Zn(CF_3SO_3)_2$, among others.[16,162] One of the primary advantages of utilizing aqueous electrolytes is their cost-effectiveness, along with a significantly reduced risk of combustion and explosion compared to organic electrolytes, ultimately enhancing the safety of the associated battery systems. To further optimize the performance of these electrolytes, researchers often introduce additives into the mix. These additives may consist of a blend of salts, polymers, surfactants, inhibitors, and more. For instance, Zheng *et al.*[156] explored the incorporation of a natural additive known as gum arabic into the $ZnSO_4$-based electrolyte. The inclusion of gum arabic had the beneficial effect of inhibiting water decomposition, reducing unwanted activity, and minimizing the formation of dendrimers and by-products within the system. ZIBs have a stability of 3600 h at 2.5 mA cm^{-2} with 0.5 mA h cm^{-2}, which is far more than pure $ZnSO_4$ electrolyte (Fig. 10a). In a similar vein, Cao *et al.*[157] introduced sulfolane additives to an aqueous electrolyte, leading to a reduction in the reactivity of water molecules at the zinc anode-electrolyte interface (Fig. 10b). This, in turn, effectively suppressed the formation of dendrimers and mitigated undesirable side reactions, contributing to improved battery performance. In the VO_2//Zn full cell, a capacity retention of 81.25% was maintained after 500 cycles.

4.1.2. Non-aqueous electrolytes. However, in aqueous electrolytes, the presence of active water molecules often leads to concurrent hydrogen evolution and oxygen evolution processes. Unfortunately, these side reactions can have a detrimental impact on the electrochemical performance of ZIBs, significantly compromising their efficiency and overall effectiveness. Nonaqueous electrolytes find prominent application in ZIBs that demand both high energy density and high power density, catering to critical sectors like electric vehicles and energy storage systems. These electrolytes offer the advantage of extended voltage range and demonstrate superior performance, especially under elevated temperatures. Typically, nonaqueous electrolytes are composed of organic solvents (such as acetonitrile (AN), acetone (AC), dimethyl sulphoxide (DMSO), phosphate esters, *etc.*) and organic salts.[158,159,163–165] Their primary purpose is to serve as a medium for the efficient transport of zinc ions while exhibiting the requisite conductivity and stability to ensure optimal battery performance and safety. Researchers are actively exploring novel nonaqueous electrolyte formulations that extend beyond traditional organic solvents and salts, incorporating multifunctional additives. For example, Raza *et al.*[158] introduced a nonaqueous electrolyte incorporating *N*,*N*-dimethylformamide (DMF)-based Cu^{2+} as additives. The combined thermodynamic stability of DMF and the interfacial tailoring effect of Cu^{2+} synergistically influenced the behavior of the zinc anode, resulting in ZIBs with an extended electrochemical window (~2.45 V *vs.* Zn/Zn^{2+}), exceptional stability (1400 h), and high coulombic efficiency (~99.60%) (Fig. 10c). In a parallel effort, Ni *et al.*[159] conducted a comparative study on the electrochemical properties of zinc salts in both AN and triethyl phosphate (TEP). Their investigation revealed that these zinc salts exhibit remarkable solubility and electrochemical stability. Furthermore, the $Zn(TFA)_2$-AN-TEP electrolyte demonstrated remarkable specific density and capacity retention, underscoring its potential for enhancing the performance of ZIBs. The discharge capacity of the cell reached 104.8 mA h g^{-1} at a current density of 0.1 A g^{-1}, and the capacity retention after 1000 cycles was 71.7% (Fig. 10d).

4.1.3. Aqueous–nonaqueous hybrid electrolytes. Presently, the exploration of aqueous–nonaqueous hybrid electrolytes has emerged as a prominent focus in the realm of ZIBs research. These hybrid electrolytes typically entail a blend of aqueous and nonaqueous components, offering a strategic approach to mitigating the limitations inherent to each type of electrolyte while enhancing overall battery performance This innovative electrolyte design aims to harness the

synergistic advantages of both aqueous and nonaqueous electrolytes, thereby tailoring them to meet the specific performance requirements of ZIBs. In a study, Geng *et al.*[160] developed a novel hybrid electrolyte incorporating ethylene glycol (EG) and $ZnCl_2$. This hybrid electrolyte leveraged strong interactions between EG molecules and Zn^{2+}, resulting in the formation of a complex that served as a solid electrolyte diaphragm on the zinc anode. This innovation led to the creation of a highly safe and stable ZIBs system, the prepared polyaniline//Zn cells still achieved 78% capacity retention after 10 000 cycles (Fig. 10e). Similarly, Meng *et al.*[161] introduced an electrolyte that combines AN and water as co-solvents, demonstrating its applicability across various battery systems. The resultant electrolyte interface, formed by AN, effectively controlled zinc deposition, prevented hydrogen formation, and notably enhanced the cycling stability and rate performance, Zn//Zn symmetric cell with hybrid electrolyte has an ultra-long cycle of 2100 hours at a current density of 5 mA cm^{-2} (Fig. 10f). In a recent breakthrough, Mei *et al.*[166] unveiled an organic-aqueous hybrid electrolyte incorporating $Zn(OTf)_2$-TEP/H_2O. This formulation showcased the remarkable capability to enable the anode to exhibit outstanding zinc storage capacity, consequently elevating the stability of ZIBs to new heights. The capacity at a current density of 0.5 A g^{-1} was 117.8 mA h g^{-1}, and the capacity retention after 4000 cycles reached 78.6%. The advent of these hybrid electrolytes signifies a pivotal advancement in ZIBs technology, offering tailored solutions to overcome existing challenges and elevating the prospects for safer, more stable, and higher-performing energy storage systems.

4.2. Solid electrolyte

The surge in demand for flexible ZIBs in the context of flexible electronic devices has fueled extensive research into the development of appropriate solid electrolytes.[167–169] In contrast to liquid electrolytes, solid electrolytes offer multiple

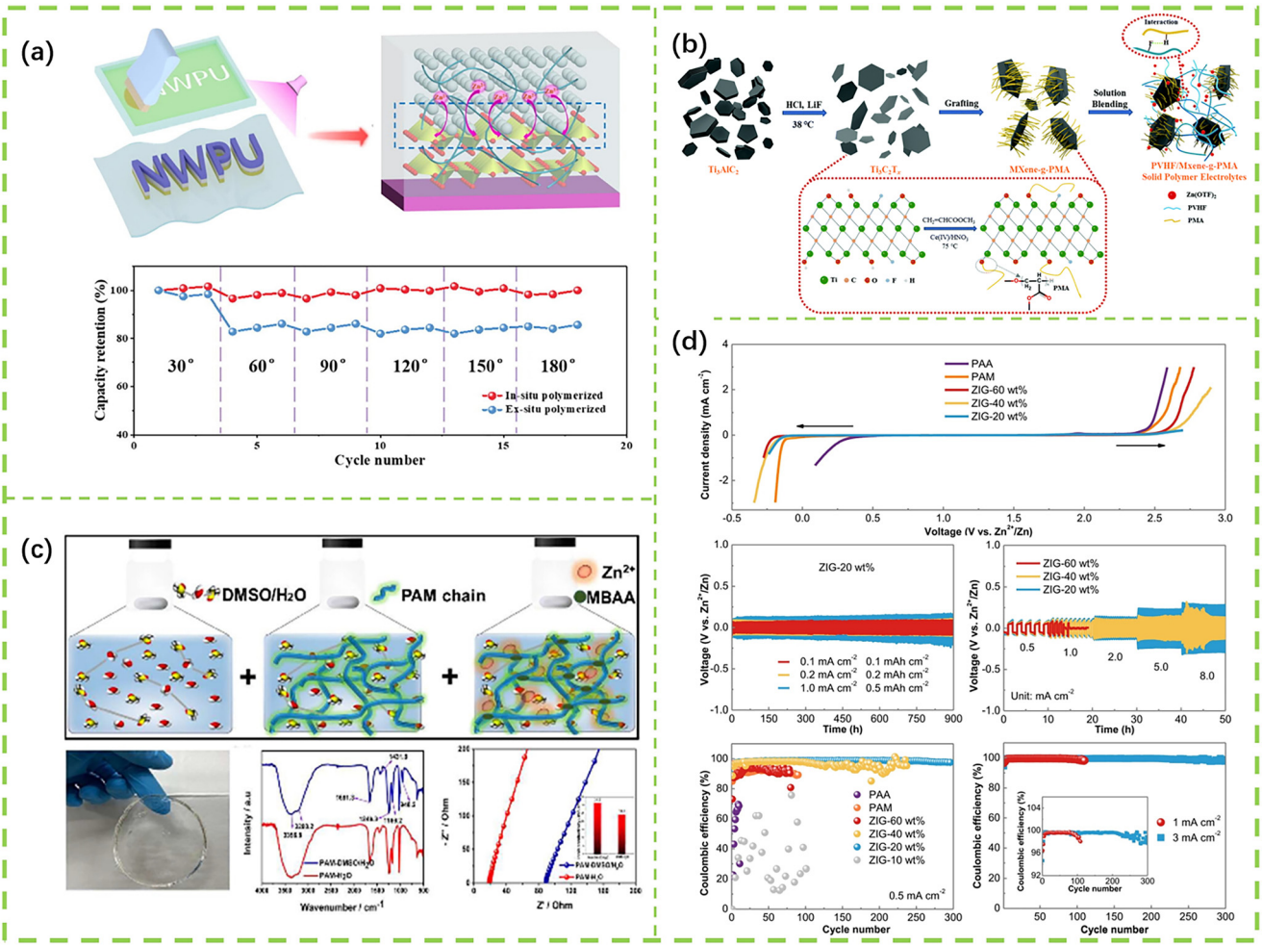

Fig. 11 Solid electrolyte: (a) fabricate flexible all-solid-state ZIBs through stencil printing combined with UV-assisted curing technology. Reproduced with permission from ref. 173. Copyright 2023, Elsevier Ltd. (b) A solid polymer electrolyte based on poly (methyl acrylate) grafted MXenes. Reproduced with permission from ref. 171. Copyright 2022, Elsevier Ltd. (c) DMSO was combined with H_2O to prepare a gel electrolyte (PAM-DMSO/H_2O). Reproduced with permission from ref. 174. Copyright 2023, Elsevier Ltd. (d) A lean water hydrogel electrolyte. Reproduced with permission from ref. 175. Copyright 2023, Elsevier Ltd.

advantages. They not only eliminate the issue of electrolyte leakage but also function as a diaphragm to avoid cathode and anode contact while transporting zinc ions. Additionally, solid electrolytes possess distinct mechanical properties that enable them to withstand various mechanical operations such as stretching, bending, and twisting. In terms of physical state, solid electrolytes are typically categorized into two main types: all-solid-state electrolytes and quasi-solid-state electrolytes applied to solid-state and quasi-solid-state batteries.[17,170–172]

4.2.1. All-solid-state electrolytes. The all-solid-state electrolyte comprises polymer as the substrate, organic/inorganic zinc salt to provide Zn^{2+}, and contains no liquid solvent. This configuration leads to a substantial reduction in undesirable side reactions caused by active water molecules and effectively curtails the growth of zinc dendrites. Consequently, all-solid-state ZIBs exhibit heightened stability and safety.[176] Nonetheless, the primary impediments to its advancement lie in the limited conductivity of the all-solid-state electrolyte and suboptimal electrode contact. To address these challenges, a variety of approaches have been explored to enhance the performance of all-solid-state electrolytes. Including materials design,[166,177] interface engineering[173,178] and so on. For instance, Chen *et al.*[171] achieved significant improvement by incorporating poly(methyl acrylate) highly grafted MXene into poly(vinylidene fluoride-*co*-hexafluoropropylene), leading to a notable enhancement in ionic conductivity (2.69×10^{-4} S cm^{-1}). This innovative modification effectively mitigates dendrite formation and side reactions, and a capable of stable operation from −35 °C to 100 °C (Fig. 11a). Another noteworthy advancement comes from the work of Bu *et al.*,[173] who developed a robustly bonded cross-linked anode/electrolyte interface through ultraviolet-assisted curing. This interface not only amplifies the ion transport pathway between the all-solid-state electrolyte and the electrode but also mitigates the issue of electrolyte detachment during various deformations, the prepared ZIB was able to achieve a capacity of 165.9 mA h g^{-1}. Consequently, this approach substantially elevates the cycling stability and mechanical resilience of all-solid-state ZIBs (Fig. 11b).

4.2.2. Quasi-solid-state electrolytes. Quasi-solid-state electrolytes have garnered significant attention from researchers due to their superior interfacial compatibility with electrodes when compared to all-solid-state electrolytes. These quasi-solid-state electrolytes typically manifest as gel polymer electrolytes, comprising a blend of liquid electrolyte and polymer matrix.[174,175,179] These electrolytes demonstrate commendable attributes, including high ionic conductivity and flexibility. Furthermore, they typically exhibit enhanced stability at elevated temperatures and have been engineered to include self-healing and thermo-reversible functionalities. These features render ZIBs exceptionally well-suited for applications in high-temperature environments. In pursuit of meeting the stringent demands of ZIBs, efforts have been directed towards refining quasi-solid-state electrolytes

Table 4 The key parameters for cathode, anode and electrolyte

Type	Material	Specific capacity	Cycle life (retention)	Notable features
Anode	Zn metal	~820 mAh g^{-1} (theoretical); practical ~300 mAh g^{-1}	100–300 cycles (rapid degradation if unprotected)	Dendrite formation; requires additives/coatings for stability
Anode	Zn–Al alloy[18]	~320 mAh g^{-1} (at 0.5 mA cm^{-2})	1000+ hours in symmetric cell (>80% capacity retention)	Lamellar alloy structure suppresses dendrites and prolongs Zn plating life
Anode	Zn@carbon foam[15]	~300 mAh g^{-1} (at 2 mAh cm^{-2})	3000 h stable Zn plating (no shorting)	3D porous carbon host ensures uniform Zn deposition
Cathode	α-MnO_2 (nanowire)[27]	280 mAh g^{-1} (0.3 A g^{-1})	94% capacity after 2000 cycles	$MnSO_4$ additive used to suppress Mn dissolution
Cathode	V_2O_5 (hydrated)[30]	350 mAh g^{-1} (0.1 A g^{-1})	91% after 4000 cycles (5 A g^{-1})	Pre-inserted H_2O in structure enables fast Zn^{2+} diffusion and stability
Cathode	ZnHCF (Prussian blue analog)[42]	~65 mAh g^{-1} (0.1 A g^{-1})	80% after 5000 cycles (5 C rate)	Open framework with minimal strain; excellent high-rate capability
Cathode	PANI (polymer)[45]	~110 mAh g^{-1} (0.5 A g^{-1})	85% after 1000 cycles	Conductive polymer, stores charge *via* protonation/deprotonation; requires carbon composite for conductivity
Cathode	Mo_6S_8 (Chevrel)[51]	~100 mAh g^{-1} (0.2 A g^{-1})	90% after 400 cycles	3D cluster framework allows rapid Zn^{2+} intercalation with low strain
Electrolyte	2 M $ZnSO_4$ (aqueous)	—	—	Baseline electrolyte; pH ~4–5; voltage window ~1.8 V; prone to Zn dendrites and HER at Zn anode
Electrolyte	"Water-in-salt" (*e.g.* 30 m $ZnCl_2$)[16]	—	—	Super-concentrated electrolyte extends stability window to ~2.3 V; suppresses water activity and dendrites; higher viscosity/cost
Electrolyte	$Zn(OTf)_2$-Acetonitrile[160]	—	—	Non-aqueous/aqueous hybrid electrolyte; widens voltage window, eliminates water-induced side reactions; flammable organic content
Electrolyte	PVA–$ZnSO_4$ gel (quasi-solid)[4]	—	95% after 500 cycles (bendable cell)	Gel polymer electrolyte with ionic conductivity ~10^{-3} S cm^{-1}; improves safety and enables flexible ZIB designs

through compositional modifications and the introduction of multifunctional fillers.[180–182] For instance, Kimilita *et al.*[174] prepared a gel-like electrolyte by combining DMSO with H_2O, and by adjusting the ratio of DMSO/H_2O, the electrolyte exhibited excellent interfacial compatibility and ionic conductivity, the prepared Al-VOH/PAM-DMSO/H_2O/Zn full cell exhibited a high capacity of 559.0 mA h g^{-1} and achieved a stability of 2000 cycles, which greatly improved the electrochemical and mechanical properties of ZIBs (Fig. 11c). Furthermore, Wang *et al.*[175] have engineered a lean hydrogel electrolyte. In this design, the water lubrication mechanism within the electrolyte amplifies zinc ion conductivity (2.6×10^{-3} S cm^{-1}) while enhancing the stability of water molecules under a 20% lean-water content. This innovation effectively broadens the electrochemical window of ZIBs, and the electrochemical stability up to 4000 cycles at 5C (Fig. 11d).

4.3. Summary of this chapter

Electrolytes play a critical role in zinc-ion batteries (ZIBs), influencing ion transport, stability, and interfacial compatibility. Aqueous electrolytes (*e.g.*, $ZnSO_4$, $Zn(CF_3SO_3)_2$) are cost-effective and safe but suffer from water-induced side reactions like hydrogen evolution and dendrite growth, which additives (*e.g.*, gum arabic, sulfolane) can mitigate. Non-aqueous electrolytes (*e.g.*, AN, DMF-based systems) offer wider voltage windows and high-temperature stability but face challenges in ionic conductivity and interfacial compatibility. Hybrid electrolytes (aqueous/non-aqueous blends, *e.g.*, EG-$ZnCl_2$, AN-H_2O) combine the advantages of both, enhancing cycling stability and suppressing parasitic reactions. Solid-state electrolytes (all-solid and quasi-solid) eliminate leakage and dendrite issues while enabling flexible ZIBs. All-solid-state electrolytes (*e.g.*, polymer-MXene composites) improve safety but require enhanced conductivity, whereas quasi-solid gels (*e.g.*, PAM-DMSO/H_2O hydrogels) balance ionic transport and mechanical flexibility. Future research should focus on optimizing electrolyte formulations (additives, hybrid systems) and interfacial engineering to achieve high-performance, durable, and scalable ZIBs. In addition, we summarize the key parameters of the cathode, anode, and electrolyte in Table 4 to achieve more effective matching for higher performance of zinc-ion batteries.

5. Working mechanism for ZIBs

Research on the working mechanism of ZIBs is of paramount importance, which not only helps in optimizing their electrochemical performance, such as energy density and cycling stability, but also provides a foundation for developing safer and more sustainable energy storage solutions. Understanding how zinc ions interact with electrode materials during charge and discharge can lead to the design of novel electrode materials with enhanced conductivity and capacity.[19] Additionally, it aids in identifying degradation mechanisms and developing strategies to mitigate them, thereby extending the lifespan of the batteries.[33] As for most anode side in ZIBs, the electrochemical process entails a straightforward reversible redox reaction of Zn ($Zn^0 - 2e^- \rightleftharpoons Zn^{2+}$).[19] However, the electrochemical reaction for the cathode would be much more complex. According to the redox chemistry, the working mechanisms can be categorized as cationic redox, anionic redox, and redox of active functional groups.

5.1. Cationic redox

Cationic redox refers to the reduction/oxidation of transition metals, such as $Mn^{4+} \rightleftharpoons Mn^{3+} \rightleftharpoons Mn^{2+}$, $Fe^{3+} \rightleftharpoons Fe^{2+}$ and so on. Given that Zn^{2+} (0.74 Å) have a similar ionic radius to that of Li^+ (0.76 Å), which can be favorable for the insertion and extraction of carriers within the host material. Due to the existence of solvation effect, Zn^{2+} typically undergoes hydration with six water molecules to form hydrated cations with a radius of 4.3 Å, which means large interlayer distances and/or tunnel sizes should be considered for cathode material design. Remarkably, the surrounded H_2O can be capable of effectively shielding the electrostatic interactions of the intercalated Zn^{2+}, facilitating the insertion and extraction.

In the mildly acidic electrolytes, the directional movement of zinc ions would be often accompanied with the movement of protons, which may or may not be a simultaneous process. This process largely depends on the choice of material system. Chen *et al.* demonstrated that H^+ and Zn^{2+} could be simultaneously inserted and extracted into/from the $NaV_3O_8{\cdot}1.5H_2O$ cathode, which renders excellent electrochemical performance.[112] For MnO_2 cathodes, the reversible insertion and extraction of H^+ and Zn^{2+} have been shown to be a two-step process. Wang and colleagues[76] proposed this stepwise mechanism based on an electrodeposited ε-MnO_2. From the galvanostatic intermittent titration technique (GITT) curve, the rapid ionic diffusion with minimal voltage fluctuation indicated the intercalation of H^+. As the depth of discharge continues, the significant overpotential corresponded to the Zn^{2+} intercalation due to its slower diffusion rate. It is worth noting that the insertion of H^+ increases the concentration of OH^- near the cathode, leading to the precipitation of $ZnSO_4[Zn(OH)_2]_3{\cdot}xH_2O$ flakes on the cathode surface. The extraction of H^+ after recharging dissolves the $ZnSO_4[Zn(OH)_2]_3{\cdot}xH_2O$ products.

5.2. Anionic redox

The redox process of anions, such as oxygen, sulfur, and nitrogen, has been observed as an accompanying mechanism in ZIBs. Chen and his team[101] discovered a dual-redox process involving both cationic V and anionic oxygen using a $VOPO_4$ cathode. The oxidation of oxygen occurred at the end of the first charge, indicating the oxidation of lattice oxygen from O^{2-} to O^{1-}. In reverse, O^{1-} was reduced back to O^{2-} during the subsequent discharge from 2.1 V to 1.7 V. The reduced oxygen intensity in the X-ray absorption spectra (SXAS) at the fully discharged state was attributed to the reduction of V. Conversely, the stronger signals at the fully charged state compared to the initial state indicated the oxidation of oxygen. It is important to note that the oxygen redox chemistry not only

contributes additional specific capacity but also increases the average working voltage of Zn/$VOPO_4$ batteries. It is important to note that the oxygen redox chemistry not only contributes additional specific capacity but also increases the average working voltage of Zn/$VOPO_4$ batteries. A similar dual-ion mechanism was also observed in a surface-oxidized vanadium nitride (VN_xO_y) cathode, which involved a simultaneous reversible reaction of cationic redox ($V^{3+} \leftrightarrow V^{2+}$) during Zn^{2+}/H^+ de-/intercalation and pseudo-capacitance-like surface anionic redox ($N^{3+} \leftrightarrow N^{2+}$) during OH^- release/uptake.[183] Notably, the lower electronegativity of nitrogen compared to oxygen can weaken the ionic bonds between Zn^{2+} and oxygen, thereby enabling rapid and reversible diffusion of Zn^{2+}. As a result, the VN_xO_y cathode exhibited outstanding rate performance of 200 mA h g^{-1} at 30 A g^{-1} and superior 2000-cycling durability.

5.3. Redox of active functional groups

In recent years, researchers have explored a variety of organic compounds with abundant functional groups as alternative cathodes for ZIBs, such as PANI,[184] quinone,[185] calix[4]quinone (C4Q),[151] sulfur heterocyclic quinone dibenzo[*b*,*i*]thianthrene-5,7,12,14-tetraone[186] and pyrene-4,5,9,10-tetraone (PTO).[187] The reaction mechanism of these organic compounds typically involves the redox activity of functional groups within their chain structure, such as C═N– and carbonyl groups (C═O).[188] For example, in PANI, the C═N^-– and protonated C═NH^+– groups are recognized as the electrochemically active sites for Zn^{2+} storage.[189] During the initial discharge, the protonated ═NH^+ groups are reduced to –NH–. At the same time, the C═N– in the polymer backbone is reduced to electronegative –N– species, which can attract Zn^{2+}. After partial charging, both the –NH– and –N– groups return to their original ═NH^+– and C═N– states, respectively. It is worth noting that the surplus –NH– groups in PANI can be further oxidized to ═NH^+– when fully charged. In addition to nitrogen-containing species, the electronegative oxygen in C═O groups can also serve as active centers to coordinate with Zn ions. Thanks to the abundance of C═O active centers on the surface, each C4Q molecule can coordinate with three Zn^{2+}.[151] Although still in the early stages, these innovative preliminary studies may

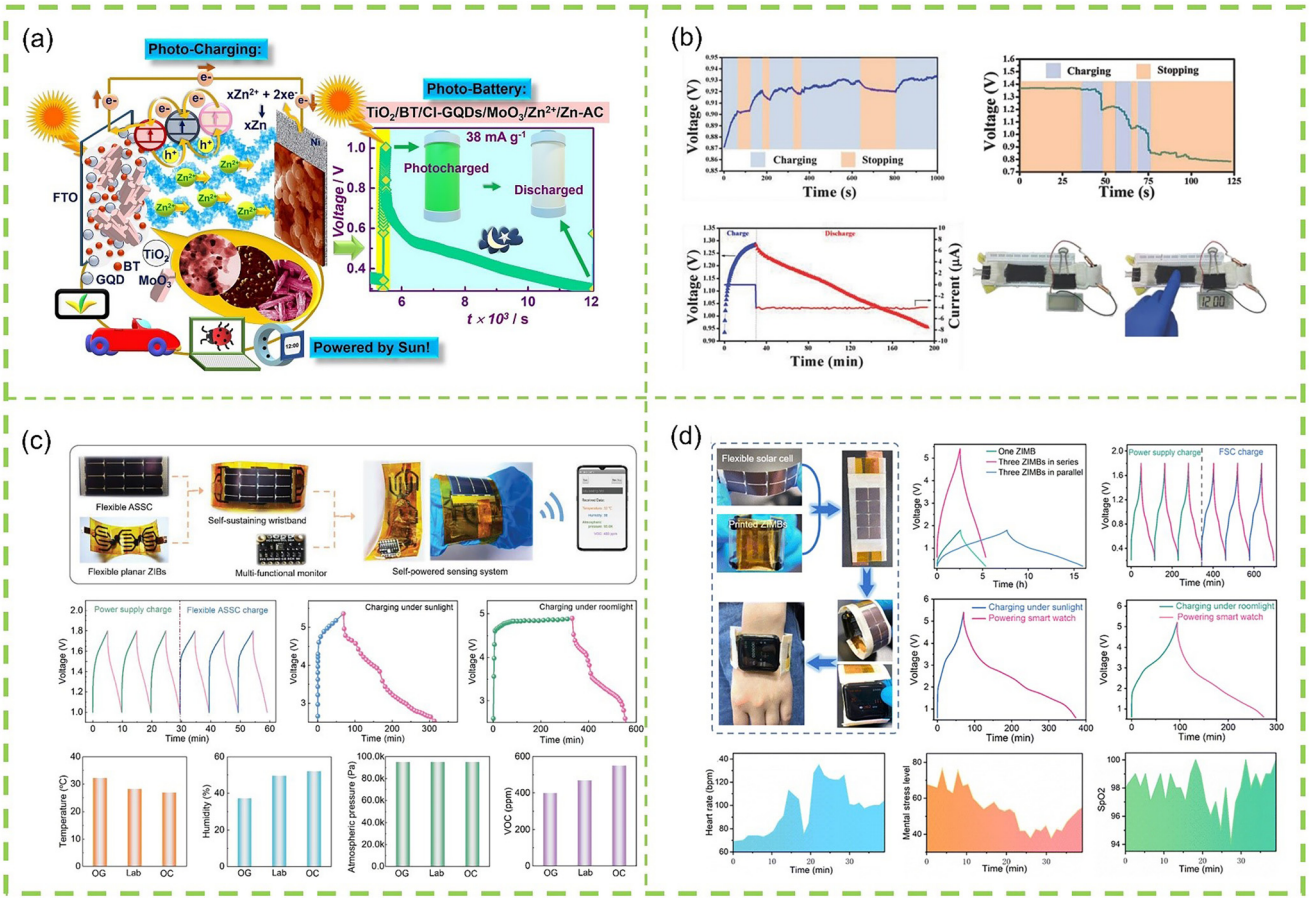

Fig. 12 Applications in energy harvesting and energy utilization: (a) a unique rapid-charging photo-battery of TiO_2/BT/Cl-GQDs/MoO_3-NRs/Zn^{2+}/Zn-AC to harvest light energy. Reproduced with permission from ref. 190. Copyright 2023, Elsevier Ltd. (b) Integration and the charging of the flexible ZIB by the triboelectric nano-generator fabric. Reproduced with permission from ref. 191. Copyright 2018, WILEY-VCH Verlag GmbH & Co. KGaA, Weinheim. (c) Flexible planar ZIBs for a self-powered wearable sensing system. Reproduced with permission from ref. 192. Copyright 2023, Wiley-VCH Verlag GmbH & Co. KGaA, Weinheim. (d) Printed ZIBs for a self-powered smart watch. Reproduced with permission from ref. 193. Copyright 2023, Royal Society of Chemistry.

pave a new way for the development of novel organic compounds with rich functional groups that can actively participate in redox reactions with Zn^{2+}.

5.4. Summary of this chapter

The working mechanisms of zinc-ion batteries (ZIBs) primarily involve three redox pathways: cationic redox, anionic redox, and redox of active functional groups. The anode typically undergoes a simple Zn^{2+} plating/stripping process ($Zn^0 \leftrightarrow Zn^{2+}$), while cathode reactions are more complex. Cationic redox involves transition metal valence changes (*e.g.*, Mn^{4+}/Mn^{3+}, V^{5+}/V^{4+}), often coupled with H^+/Zn^{2+} co-intercalation, influenced by solvation effects and host material structure. Anionic redox (*e.g.*, O^{2-}/O^-, N^{3-}/N^{2-}) contributes additional capacity and higher voltages, as seen in $VOPO_4$ and VN_xO_y cathodes. Organic cathodes leverage redox-active functional groups (*e.g.*, C═O, C═N) for Zn^{2+} coordination, enabling high capacity but facing challenges in stability. Understanding these mechanisms is crucial for optimizing electrode design, enhancing ion transport, and mitigating degradation, paving the way for high-performance, sustainable ZIBs.

6. Applications of zinc-ion batteries

Leveraging their inherent advantages including exceptional safety profiles, abundant zinc reserves, cost-efficiency, and remarkable energy density, ZIBs have emerged as a frontrunner in next-generation energy storage technologies with unparalleled research and development potential. This electrochemical energy storage system demonstrates transformative capabilities across diverse application fields, with continuous technological breakthroughs driving their rapid deployment in innovative configurations that yield impressive operational outcomes.[11]

As global demand surges for sustainable energy solutions, ZIBs distinguish themselves through their unique compatibility with energy harvesting technologies – a critical advantage for ensuring reliable power supply integration. Their superior energy capture capabilities span multiple domains including photoelectric conversion, mechanical energy harvesting, and thermal energy utilization, with experimental systems already achieving groundbreaking performance. Kaur *et al.*[190] revolutionized solar integration by developing a dual-functional ZIB system incorporating natural beetroot dye and chlorine-doped quantum dots, achieving exceptional 1 V charging under solar exposure with 240 mA h g^{-1} discharge capacity. Concurrently, Wang *et al.*[191] demonstrated the mechanical energy superiority of ZIBs through a textile-integrated triboelectric nanogenerator system that converts human motion into stored energy, boosting battery voltage by 37% while delivering 10.9 μAh discharge capacity-a testament to their mechanical–electrical conversion efficiency (Fig. 12).

The operational versatility of ZIBs shines particularly in flexible energy solutions, where their mechanical resilience and high energy retention enable transformative wearable applications. Cai *et al.*[192] engineered a self-powered sensing system combining printed flexible ZIBs with solar cells, overcoming intermittent renewable supply limitations while enabling continuous environmental monitoring. Yan *et al.*[193] further extended these advantages through 3D-printed micro-batteries integrated into smart wearables, achieving full-day physiological monitoring capabilities. Beyond portable electronics, ZIBs demonstrate exceptional scalability for industrial applications including seawater electrolysis, leveraging their superior corrosion resistance and catalytic efficiency in hydrogen production.

The strategic advantages of ZIBs become particularly pronounced in electric vehicle (EV) and grid-scale applications, where they outpace conventional LIBs through multiple performance parameters. Their aqueous electrolyte systems eliminate combustion risks while providing enhanced thermal stability – critical safety advantages for collision-prone EV applications. Coupled with rapid charging capabilities and theoretical energy densities exceeding 400 W h kg^{-1}, ZIBs present a formidable alternative to LIBs in transportation electrification. For grid-scale deployment, ZIBs offer unmatched economic and operational benefits: Their low-cost zinc-based chemistry enables massive energy arbitrage capabilities, effectively balancing supply–demand fluctuations while providing emergency backup resilience. These grid systems capitalize on ZIBs' unique ability to store surplus renewable energy during off-peak periods for high-value discharge during demand peaks, significantly improving grid reliability and operational economics.

The commercial trajectory of ZIBs reflects their compelling value proposition, with global markets projected to expand from $0.2 billion to $28.1 billion by 2030. Their commercialization strengths stem from three core advantages: (1) abundant zinc reserves ensuring material security and price stability; (2) simplified recycling processes enabling >95% metal recovery rates; (3) inherent non-flammability addressing critical safety concerns in energy storage. Current production optimizations focus on enhancing their natural advantages through advanced electrode architectures and electrolyte formulations, targeting 50% cost reductions *versus* LIBs while maintaining competitive energy densities.

While technical challenges in zinc dendrite suppression and electrolyte optimization remain, ZIBs' fundamental advantages position them as a cornerstone technology for sustainable energy transitions. Their development directly supports global decarbonization goals through reduced resource intensity (60% lower than LIBs in lifecycle assessments) and enhanced renewable integration capabilities. As research breakthroughs continue to amplify their innate strengths, ZIBs are poised to redefine energy storage paradigms across consumer electronics, transportation, and grid infrastructure sectors-establishing zinc as the keystone material for next-generation electrochemical storage solutions.

7. Bright prospects of ZIBs

Zinc-ion batteries offer a combination of high safety, low cost, environmental friendliness, excellent electrochemical performance, and broad applicability, making them highly promising for future energy storage applications. With ongoing technological advancements, ZIBs are poised to replace traditional battery technologies in various fields, providing significant support for global energy transitions and sustainable development. The specific advantages would be demonstrated as following:

(1) High safety

ZIBs are considered as the ideal energy-supply equipment for wearable electronics. In the standard configuration, they utilize non-noble materials such as zinc foil, carbon-based materials, and inorganic salts, combined with aqueous electrolytes, which are inherently less reactive and more stable than the organic electrolytes used in LIBs. This significantly reduces the risk of thermal runaway, combustion, or explosion, which are common safety concerns in lithium-based systems.[170]

(2) Cost-effectiveness

ZIBs offer significant cost advantages over LIBs in general. Firstly, the abundance of zinc in the Earth's crust is approximately four times that of lithium, making zinc a more readily available and cheaper raw material. The price of zinc (0.5–1.5$ per lb) is much lower than that of lithium (8–11$ per lb).[194] Additionally, ZIBs can be manufactured in open-air environments, whereas LIBs often require inert atmospheres for production, which increases the manufacturing cost. Furthermore, the electrolytes used in ZIBs are typically aqueous and less expensive compared to the organic electrolytes used in LIBs. These combined factors make ZIBs a more cost-effective energy storage solution, especially for cost-sensitive devices.

(3) Compatibility

The manufacturing processes for ZIBs are similar to those for LIBs. First of all, both ZIBs and LIBs utilize electrodes that can be fabricated using common methods such as slurry coating, drying, and calendaring. The active materials for ZIBs (*e.g.*, zinc metal for the anode and various transition metal oxides or Prussian blue analogs for the cathode) can be processed into slurries and coated onto current collectors in a manner similar to that used for LIB electrodes. And ZIBs typically use aqueous electrolytes, the principles of electrolyte formulation and handling are analogous to those in LIBs. The aqueous electrolytes used in ZIBs can be integrated into existing battery assembly lines with minimal modifications, as they are compatible with the same types of separators and packaging materials used in LIBs. At the same time, the assembly of ZIBs follows similar steps to those of LIBs, including stacking or winding of electrodes, electrolyte filling, and cell sealing. The flexible configurations of ZIBs, such as planar or cable structures, can be adapted to existing manufacturing equipment used for LIBs, making it feasible to switch between the two battery types with minimal investment in new machinery.[195–198] Moreover, ZIBs offer the intrinsic potential for scalability and industrial compatibility. The manufacturing processes for ZIBs can be scaled up using the same principles as those for LIBs. Techniques like roll-to-roll processing, which are commonly used for LIB production, can also be applied to ZIBs, ensuring that large-scale production is feasible and cost-effective.

Overall, the combination of safety, cost-effectiveness, and compatibility with the existing industrial foundation makes ZIBs a highly attractive option for next-generation energy storage solutions.

8. Main challenges and possible solutions

ZIBs have garnered significant attention as a promising alternative for sustainable energy storage, thanks to their numerous advantages. However, despite these promising attributes, ZIBs face several challenges that need to be addressed for their practical application. As for anode, one significant concern is the formation of zinc dendrites during repeated charge–discharge cycles, which can lead to short circuits and reduced battery lifespan. This problem would be exacerbated by the inhomogeneous deposition of zinc ions, causing uneven growth on the anode surface. Additionally, the aqueous electrolytes used in ZIBs can suffer from a narrow electrochemical stability window, leading to hydrogen evolution reactions and corrosion of the zinc anode. These side reactions not only decrease the coulombic efficiency but also result in the formation of by-products that disturb the uniform deposition of zinc. Another challenge lies in the cathode materials, which often experience dissolution of active materials and structural degradation during cycling, leading to poor rate capability and cycling stability. For instance, transition metal-based compounds like manganese and vanadium oxides, as well as Prussian blue analogs, are prone to dissolution of metal ions, further compromising their performance. Moreover, our understanding of the electrochemical mechanisms of ZIBs would be still incomplete and inaccurate, and the reasons for this would be varied. Firstly, the aqueous electrolytes commonly used in ZIBs may trigger various side reactions, which not only brings difficulties to the phase analysis of electrochemical processes, but also impedes the detection of target products. Besides, the solvation and de-solvation processes of zinc ions are intricate, which would be difficult to perceive due to the restricted characterization techniques.

Herein, we propose some perspectives in view of the issues for ZIBs as shown in Fig. 13:

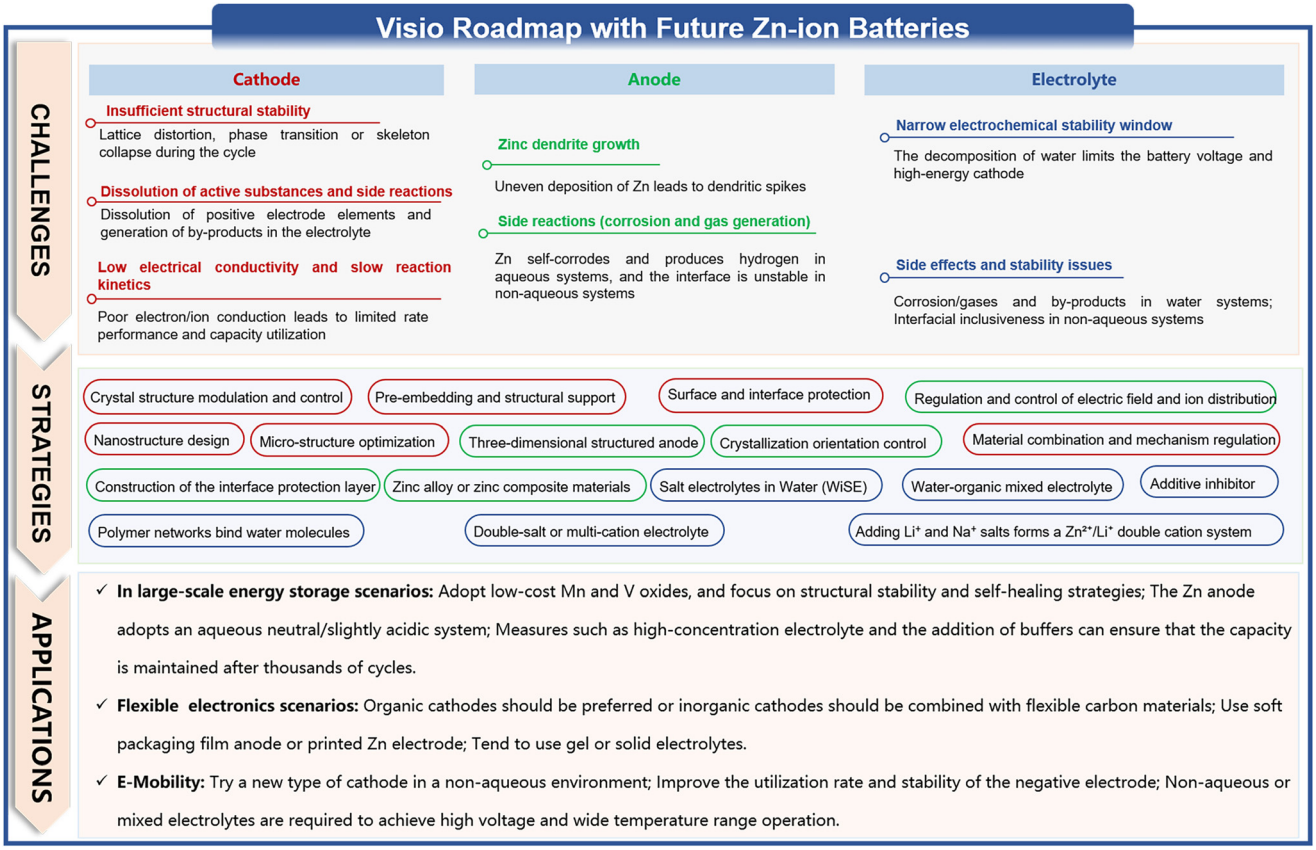

Fig. 13 The visio roadmap with future Zn-ion batteries.

(1) Design and optimization of anode materials

As discussed above, surface modification with protective layers, such as carbon-based materials, polymers, or metal oxides, can effectively inhibit zinc dendrite growth and corrosion, thereby improving the anode's stability and cycle life. And the significance of structural design would be taken into account as well, including the establishment of three-dimensional porous frameworks and conductive substrates, to promote uniform zinc deposition and reduce local current density. While these standard modification techniques merit the scrutiny of scholars, the influence of different components in ZIBs, particularly the electrolyte, on the anode should not be overlooked. Improving the compatibility of electrolyte and anode material is also an important direction worth studying in the future.

(2) Advanced electrolyte design

The development of aqueous electrolyte and solid electrolyte is never a contradictory relationship, and it is the most important to choose the appropriate electrolyte system for the actual service environment of the battery. As for aqueous electrolyte, future research should focus on expanding the electrochemical stability window and minimizing adverse reactions as much as possible. The expertise can be gained from the design strategy of LIBs, such as establishing water-in-salt one. When facing flexible wearable devices or implantable devices, solid phase electrolytes are bound to become the best choice for energy sources due to their excellent safety performance. In this moment, establishing appropriate safety standards and researching on failure mechanisms in real service environments should be the top priority.

(3) Design and optimization of cathode materials

The choice of cathode materials is obviously more than that of anode materials, offering researchers diverse choices but clearly escalating the workload. Future studies will focus not only on improving current materials but also on searching and screen more advanced ones *via* high-throughput computing method or artificial intelligence technology. It is worth mentioning that the optimization of the cathode material still needs to consider compatibility with other components, such as the electrochemical platform of the cathode material within the electrochemical window of the electrolyte and compatibility with the anode material capacity output.

(4) In-depth understanding of the electrochemical mechanism

By delving into their fundamental electrochemical processes, researchers can further optimize performance, enhance safety, and extend cycle life, ultimately making ZIBs more competitive in the market, which would be crucial for

developing cost-effective and sustainable energy storage solutions that can support the growing demand for renewable energy, reduce dependence on fossil fuels, and contribute to global energy security. However, the exploration of electrochemical mechanisms is often inseparable from advanced characterization techniques and *in situ* characterization methods, which is an interdisciplinary matter that often involves the development of devices.

9. Conclusion

ZIBs are promising as sustainable alternatives in the realm of energy storage. The urgent global need for decarbonization, emphasized in the introduction, underscores the significance of advanced Electrical Energy Storage (EES) systems. Throughout the paper, we meticulously investigate the various components of ZIBs, including anode materials such as metallic zinc, carbon-based structures, and transition metal oxides/sulfides/phosphides. Simultaneously, our analysis delved into cathode materials, ranging from transition metal oxides to organic cathode materials and emerging cathode nanomaterials, emphasizing recent advancements and challenges in their applications.

The pivotal role of electrolyte materials in determining battery performance was dissected, considering both liquid and solid electrolytes. Understanding the nuances of these components is vital, as highlighted in our detailed examination. Through this exploration, it becomes evident that ZIBs offer distinct advantages, notably their safety, high energy density, and eco-friendly attributes, owing to the abundance and low cost of zinc.

This paper serves as a significant contribution to ongoing discourse on energy storage technologies. By elucidating the current state of ZIB technology and its potential future trajectories, we provide researchers, policymakers, and industry stakeholders with valuable insights. The discussion on fundamental operating mechanisms, coupled with innovative approaches in electrode and electrolyte materials, illuminates a path toward overcoming challenges such as low cycle life and energy efficiency. Additionally, our focus on potential applications and market growth, especially in stationary energy resources, outlines a tangible future for ZIBs in the energy landscape.

As we venture into an era where sustainable energy solutions are imperative, the knowledge encapsulated in this review propels the development of ZIBs, offering a viable and competitive avenue for the future of energy storage. With continuous advancements, collaborative efforts, and a keen focus on addressing existing limitations, ZIBs stand poised to revolutionize the energy storage sector, steering us toward a more sustainable and environmentally conscious future.

Data availability

This review article does not generate new data. All data and information discussed are derived from previously published studies, which are appropriately cited in the manuscript.

Author contributions

Z. Chen, L. Zhang and T. Yu wrote the paper. H. Yang, Zonglun Ye, Y. Wang, B. Zheng, Y. Sun, D. Wang, G. Xu and R. Li sorted out the relevant literature. Y. Wang contributed contents to the Conclusion. W. Gao, Y. Lu, and X. Wang reviewed and revised the paper. W. Gao, R. Li, Y. Lu and X. Wang proposed the concept and the structure of this review.

Conflicts of interest

The authors declare that they have no known competing financial interests or personal relationships that could have appeared to influence the work reported in this paper.

Acknowledgements

This review is supported by the China Postdoctoral Science Foundation (No. 2021M691729), the National Natural Science Foundation of China (No. 52177217), and the Beijing Natural Science Foundation (No. 3212031).

References

1 W. Huang, X. Feng, X. Han, W. Zhang and F. Jiang, *Cell Rep. Phys. Sci.*, 2021, **2**, 100285.
2 Z. Zhu, T. Jiang, M. Ali, Y. Meng, Y. Jin, Y. Cui and W. Chen, *Chem. Rev.*, 2022, **122**, 16610–16751.
3 X. B. Cheng, R. Zhang, C. Z. Zhao and Q. Zhang, *Chem. Rev.*, 2017, **117**, 10403–10473.
4 M. Zhou, B. Li, J. Li and Z. Xu, *ACS ES&T Eng.*, 2021, **1**, 1369–1382.
5 P. Hu, T. Zhu, X. Wang, X. Wei, M. Yan, J. Li, W. Luo, W. Yang, W. Zhang, L. Zhou, Z. Zhou and L. Mai, *Nano Lett.*, 2018, **18**, 1758–1763.
6 P. Canepa, G. Sai Gautam, D. C. Hannah, R. Malik, M. Liu, K. G. Gallagher, K. A. Persson and G. Ceder, *Chem. Rev.*, 2017, **117**, 4287–4341.
7 K. E. K. Sun, T. K. A. Hoang, T. N. L. Doan, Y. Yu, X. Zhu, Y. Tian and P. Chen, *ACS Appl. Mater. Interfaces*, 2017, **9**, 9681–9687.
8 N. Zhang, X. Chen, M. Yu, Z. Niu, F. Cheng and J. Chen, *Chem. Soc. Rev.*, 2020, **49**, 4203–4219.
9 B. Tang, L. Shan, S. Liang and J. Zhou, *Energy Environ. Sci.*, 2019, **12**, 3288–3304.
10 Q. Ni, B. Kim, C. Wu and K. Kang, *Adv. Mater.*, 2022, **34**, 1–30.
11 J. Ming, J. Guo, C. Xia, W. Wang and H. N. Alshareef, *Mater. Sci. Eng., R*, 2019, **135**, 58–84.
12 R. Puttaswamy, H. Lee, H. W. Bae, D. Y. Kim and D. Kim, *Small*, 2024, **20**, 1–11.
13 R. He, F. Yu, K. Wu, H. X. Liu, Z. Li, H. K. Liu, S. X. Dou and C. Wu, *Nano Lett.*, 2023, **23**, 6050–6058.
14 Y. Lv, Y. Xiao, L. Ma, C. Zhi and S. Chen, *Adv. Mater.*, 2022, **34**, 1–31.
15 C. Su, X. Gao, K. Liu, A. He, H. He, J. Zhu, Y. Liu, Z. Chen, Y. Zhao, W. Zong, Y. Dai, J. Lin and H. Dong, *Green Energy Intell. Transp.*, 2023, **2**, 100126.

16 S. Huang, J. Zhu, J. Tian and Z. Niu, *Chem. – Eur. J.*, 2019, **25**, 14480–14494.
17 K. Wu, J. Huang, J. Yi, X. Liu, Y. Liu, Y. Wang, J. Zhang and Y. Xia, *Adv. Energy Mater.*, 2020, **10**, 1–32.
18 G. Yaman Uzunoglu and R. Yuksel, *Small*, 2025, **21**, 1–9.
19 H. Liu, J. G. Wang, Z. You, C. Wei, F. Kang and B. Wei, *Mater. Today*, 2021, **42**, 73–98.
20 F. Shao, Y. Huang, X. Wang, Z. Li, X. Huang, W. Huang, L. Dong, F. Kang, W. Liu and C. Xu, *Chem. Eng. J.*, 2022, **448**, 137688.
21 Y. Zhu, H. Li, Y. Rao, S. Guo and H. Zhou, *Adv. Energy Mater.*, 2024, **14**, 1–27.
22 J. Cao, D. Zhang, Y. Yue, X. Wang, T. Pakornchote, T. Bovornratanaraks, X. Zhang, Z. S. Wu and J. Qin, *Nano Energy*, 2021, **84**, 105876.
23 Y. Y. Liu, G. Q. Yuan, X. Y. Wang, J. P. Liu, Q. Y. Zeng, X. T. Guo, H. Wang, C. Sen Liu and H. Pang, *Chem. Eng. J.*, 2022, **428**, 132538.
24 F. Wu, Y. Chen, Y. Chen, R. Yin, Y. Feng, D. Zheng, X. Xu, W. Shi, W. Liu and X. Cao, *Small*, 2022, **18**, 1–9.
25 X. Xu, Y. Chen, W. Li, R. Yin, D. Zheng, X. Niu, X. Dai, W. Shi, W. Liu, F. Wu, M. Wu, S. Lu and X. Cao, *Small*, 2023, **19**, 1–8.
26 R. Li, L. Li, R. Jia, K. Jiang, G. Shen and D. Chen, *Small Methods*, 2020, **4**, 1–9.
27 X. Li, J. Qu, J. Xu, S. Zhang, X. Wang, X. Wang and S. Dai, *J. Electroanal. Chem.*, 2021, **895**, 115529.
28 S. Liu, H. Zhu, B. Zhang, G. Li, H. Zhu, Y. Ren, H. Geng, Y. Yang, Q. Liu and C. C. Li, *Adv. Mater.*, 2020, **32**, 1–10.
29 D. Zhang, J. Cao, Y. Yue, T. Pakornchote, T. Bovornratanaraks, J. Han, X. Zhang, J. Qin and Y. Huang, *ACS Appl. Mater. Interfaces*, 2021, **13**, 38416–38424.
30 L. E. Blanc, D. Kundu and L. F. Nazar, *Joule*, 2020, **4**, 771–799.
31 P. Yu, Y. Zeng, H. Zhang, M. Yu, Y. Tong and X. Lu, *Small*, 2019, **15**, 1–27.
32 S. W. D. Gourley, R. Brown, B. D. Adams and D. Higgins, *Joule*, 2023, **7**, 1415–1436.
33 D. Chen, M. Lu, D. Cai, H. Yang and W. Han, *J. Energy Chem.*, 2021, **54**, 712–726.
34 H. Luo, Q. Gou, Y. Zheng, K. Wang, R. Yuan, S. Zhang, W. Fang, Z. Luogu, Y. Hu, H. Mei, B. Song, K. Sun, J. Wang and M. Li, *ACS Nano*, 2025, **19**, 2427–2443.
35 G. Xu, Y. Zhang, M. Jiang, J. Li, H. Sun, J. Li, T. Lu, C. Wang, G. Yang and L. Pan, *Chem. Eng. J.*, 2023, **476**, 146676.
36 T. Wang, C. Li, X. Xie, B. Lu, Z. He, S. Liang and J. Zhou, *ACS Nano*, 2020, **14**, 16321–16347.
37 A. Yu, W. Zhang, N. Joshi and Y. Yang, *Energy Stor. Mater.*, 2024, **64**, 103075.
38 V. C. Ho, H. Lim, M. J. Kim and J. Mun, *Chem. – Asian J.*, 2022, **17**, e202200289.
39 Y. Liu, H. He, A. Gao, J. Ling, F. Yi, J. Hao, Q. Li and D. Shu, *Chem. Eng. J.*, 2022, **446**, 137021.
40 A. Bayaguud, Y. Fu and C. Zhu, *J. Energy Chem.*, 2022, **64**, 246–262.
41 J. Yang, R. Zhao, Z. Hu, Y. Wang, K. Zhang, Y. Wang, X. Han, A. Zhang, C. Wu and Y. Bai, *Energy Stor. Mater.*, 2024, **70**, 103449.
42 Y. Zuo, K. Wang, P. Pei, M. Wei, X. Liu, Y. Xiao and P. Zhang, *Mater. Today Energy*, 2021, **20**, 100692.
43 W. Xiong, D. Yang, T. K. A. Hoang, M. Ahmed, J. Zhi, X. Qiu and P. Chen, *Energy Stor. Mater.*, 2018, **15**, 131–138.
44 H. Kim, G. Jeong, Y.-U. Kim, J.-H. Kim, C.-M. Park and H.-J. Sohn, *Chem. Soc. Rev.*, 2013, **42**, 9011.
45 N. Diomidis and J.-P. Celis, *J. Electrochem. Soc.*, 2007, **154**, C711.
46 W. G. Sunu and D. N. Bennion, *J. Electrochem. Soc.*, 1980, **127**, 2017–2025.
47 C. Y. Jung, T. H. Kim, W. J. Kim and S. C. Yi, *Energy*, 2016, **102**, 694–704.
48 H. Yang, Z. Chang, Y. Qiao, H. Deng, X. Mu, P. He and H. Zhou, *Angew. Chem.*, 2020, **132**, 9463–9467.
49 Y. Zeng, X. Zhang, R. Qin, X. Liu, P. Fang, D. Zheng, Y. Tong and X. Lu, *Adv. Mater.*, 2019, **31**, 1–8.
50 Q. Zhang, Y. Dai, K. Zhao, C. Zhang, R. Lu, J. Li, S. Jin, L. Zhang, Q. An and L. Mai, *Nano Res.*, 2023, **16**, 11604–11611.
51 Y. Cheng, L. Luo, L. Zhong, J. Chen, B. Li, W. Wang, S. X. Mao, C. Wang, V. L. Sprenkle, G. Li and J. Liu, *ACS Appl. Mater. Interfaces*, 2016, **8**, 13673–13677.
52 W. Kaveevivitchai and A. Manthiram, *J. Mater. Chem. A*, 2016, **4**, 18737–18741.
53 M. Zhou, S. Guo, G. Fang, H. Sun, X. Cao, J. Zhou, A. Pan and S. Liang, *J. Energy Chem.*, 2021, **55**, 549–556.
54 W. Li, K. Wang, M. Zhou, H. Zhan, S. Cheng and K. Jiang, *ACS Appl. Mater. Interfaces*, 2018, **10**, 22059–22066.
55 Y. Da Cho and G. T. K. Fey, *J. Power Sources*, 2008, **184**, 610–616.
56 Z. Zhao, J. Zhao, Z. Hu, J. Li, J. Li, Y. Zhang, C. Wang and G. Cui, *Energy Environ. Sci.*, 2019, **12**, 1938–1949.
57 M. Cui, Y. Xiao, L. Kang, W. Du, Y. Gao, X. Sun, Y. Zhou, X. Li, H. Li, F. Jiang and C. Zhi, *ACS Appl. Energy Mater.*, 2019, **2**, 6490–6496.
58 M. Liu, L. Yang, H. Liu, A. Amine, Q. Zhao, Y. Song, J. Yang, K. Wang and F. Pan, *ACS Appl. Mater. Interfaces*, 2019, **11**, 32046–32051.
59 H. Li, L. Ma, C. Han, Z. Wang, Z. Liu, Z. Tang and C. Zhi, *Nano Energy*, 2019, **62**, 550–587.
60 Y. Liu, X. Zhou, R. Liu, X. Li, Y. Bai, H. Xiao, Y. Wang and G. Yuan, *ACS Appl. Mater. Interfaces*, 2019, **11**, 19191–19199.
61 Y. Cheng, H. Zhang, Q. Lai, X. Li, D. Shi and L. Zhang, *J. Power Sources*, 2013, **241**, 196–202.
62 J. F. Parker, C. N. Chervin, E. S. Nelson, D. R. Rolison and J. W. Long, *Energy Environ. Sci.*, 2014, **7**, 1117–1124.
63 X. Shi, G. Xu, S. Liang, C. Li, S. Guo, X. Xie, X. Ma and J. Zhou, *ACS Sustainable Chem. Eng.*, 2019, **7**, 17737–17746.
64 R. Yuksel, O. Buyukcakir, W. K. Seong and R. S. Ruoff, *Adv. Energy Mater.*, 2020, **10**, 1–8.
65 Y. Tian, Y. An, C. Wei, B. Xi, S. Xiong, J. Feng and Y. Qian, *ACS Nano*, 2019, **13**, 11676–11685.
66 S.-B. Wang, Q. Ran, R.-Q. Yao, H. Shi, Z. Wen, M. Zhao, X.-Y. Lang and Q. Jiang, *Nat. Commun.*, 2020, **11**, 1634.

67 L. Chang, J. Li, Q. Sun, X. Liu, X. Lu and H. Cheng, *Small*, 2024, **20**, 202408124.
68 H. Zhang, X. Liu, B. Qin and S. Passerini, *J. Power Sources*, 2020, **449**, 227594.
69 W. Liu, L. Dong, B. Jiang, Y. Huang, X. Wang, C. Xu, Z. Kang, J. Mou and F. Kang, *Electrochim. Acta*, 2019, **320**, 134565.
70 G. Li, L. Sun, S. Zhang, C. Zhang, H. Jin, K. Davey, G. Liang, S. Liu, J. Mao and Z. Guo, *Adv. Funct. Mater.*, 2024, **34**, DOI: **10.1002/adfm.202301291**.
71 J. Hao, L. Yuan, B. Johannessen, Y. Zhu, Y. Jiao, C. Ye, F. Xie and S. Qiao, *Angew. Chem.*, 2021, **133**, 25318–25325.
72 J. Huang, X. Tang, K. Liu, G. Fang, Z. He and Z. Li, *Mater. Today Energy*, 2020, **17**, 1–9.
73 T. R. Juran, J. Young and M. Smeu, *J. Phys. Chem. C*, 2018, **122**, 8788–8795.
74 X. Liu, J. Yi, K. Wu, Y. Jiang, Y. Liu, B. Zhao, W. Li and J. Zhang, *Nanotechnology*, 2020, **31**, 122001.
75 C. Xu, B. Li, H. Du and F. Kang, *Angew. Chem., Int. Ed.*, 2012, **51**, 933–935.
76 W. Sun, F. Wang, S. Hou, C. Yang, X. Fan, Z. Ma, T. Gao, F. Han, R. Hu, M. Zhu and C. Wang, *J. Am. Chem. Soc.*, 2017, **139**, 9775–9778.
77 Y. Huang, J. Mou, W. Liu, X. Wang, L. Dong, F. Kang and C. Xu, *Nano-Micro Lett.*, 2019, **11**, 49–62.
78 W. Liu, X. Zhang, Y. Huang, B. Jiang, Z. Chang, C. Xu and F. Kang, *J. Energy Chem.*, 2021, **56**, 365–373.
79 M. H. Alfaruqi, V. Mathew, J. Gim, S. Kim, J. Song, J. P. Baboo, S. H. Choi and J. Kim, *Chem. Mater.*, 2015, **27**, 3609–3620.
80 M. H. Alfaruqi, J. Gim, S. Kim, J. Song, D. T. Pham, J. Jo, Z. Xiu, V. Mathew and J. Kim, *Electrochem. Commun.*, 2015, **60**, 121–125.
81 Y. Jin, L. Zou, L. Liu, M. H. Engelhard, R. L. Patel, Z. Nie, K. S. Han, Y. Shao, C. Wang, J. Zhu, H. Pan and J. Liu, *Adv. Mater.*, 2019, **31**, 1–8.
82 Z. Azmi, K. C. Senapati, A. K. Goswami and S. R. Mohapatra, *J. Power Sources*, 2024, **613**, 234816.
83 H. Pan, Y. Shao, P. Yan, Y. Cheng, K. S. Han, Z. Nie, C. Wang, J. Yang, X. Li, P. Bhattacharya, K. T. Mueller and J. Liu, *Nat. Energy*, 2016, **1**, 1–7.
84 J. Lu, C. Zhan, T. Wu, J. Wen, Y. Lei, A. J. Kropf, H. Wu, D. J. Miller, J. W. Elam, Y. K. Sun, X. Qiu and K. Amine, *Nat. Commun.*, 2014, **5**, 1–8.
85 S. Guo, Q. Li, P. Liu, M. Chen and H. Zhou, *Nat. Commun.*, 2017, **8**, 1–9.
86 X. Wang, Z. Zhang, B. Xi, W. Chen, Y. Jia, J. Feng and S. Xiong, *ACS Nano*, 2021, **15**, 9244–9272.
87 B. Yong, D. Ma, Y. Wang, H. Mi, C. He and P. Zhang, *Adv. Energy Mater.*, 2020, **10**, 1–38.
88 B. Jiang, C. Xu, C. Wu, L. Dong, J. Li and F. Kang, *Electrochim. Acta*, 2017, **229**, 422–428.
89 J. Hao, J. Mou, J. Zhang, L. Dong, W. Liu, C. Xu and F. Kang, *Electrochim. Acta*, 2018, **259**, 170–178.
90 C. Liu, R. Li, W. Liu, G. Shen and D. Chen, *ACS Appl. Mater. Interfaces*, 2021, **13**, 37194–37200.
91 Y. H. Liu, W. H. Li, H. Y. Lü, X. X. Luo, Z. X. Huang, Z. Y. Gu, X. X. Zhao and X. L. Wu, *ACS Appl. Mater. Interfaces*, 2022, **14**, 45494–45502.
92 T. Zhou, L. Xie, Q. Han, X. Qiu, Y. Xiao, X. Yang, X. Liu, S. Yang, L. Zhu and X. Cao, *Coord. Chem. Rev.*, 2024, **498**, 215461.
93 Y. Y. Liu, L. Xu, X. T. Guo, T. T. Lv and H. Pang, *J. Mater. Chem. A*, 2020, **8**, 20781–20802.
94 Y. Zhang, S. Jiang, Y. Li, X. Ren, P. Zhang, L. Sun and H. Y. Yang, *Adv. Energy Mater.*, 2023, **13**, 1–10.
95 G. Li, L. Sun, S. Zhang, C. Zhang, H. Jin, K. Davey, G. Liang, S. Liu, J. Mao and Z. Guo, *Adv. Funct. Mater.*, 2024, **34**, 2301291.
96 N. Zhang, X. Chen, M. Yu, Z. Niu, F. Cheng and J. Chen, *Chem. Soc. Rev.*, 2020, **49**, 4203–4219.
97 T. Lv, Y. Peng, G. Zhang, S. Jiang, Z. Yang, S. Yang and H. Pang, *Adv. Sci.*, 2023, **10**, 1–49.
98 X. Li, Z. Chen, Y. Yang, S. Liang, B. Lu and J. Zhou, *Inorg. Chem. Front.*, 2022, **9**, 3986–3998.
99 C. Li, W. Wu, H. Y. Shi, Z. Qin, D. Yang, X. Yang, Y. Song, D. Guo, X. X. Liu and X. Sun, *Chem. Commun.*, 2021, **57**, 6253–6256.
100 A. K. Padhi, K. S. Nanjundaswamy and J. B. Goodenough, *J. Electrochem. Soc.*, 1997, **144**, 1188–1194.
101 F. Wan, Y. Zhang, L. Zhang, D. Liu, C. Wang, L. Song, Z. Niu and J. Chen, *Angew. Chem., Int. Ed.*, 2019, **58**, 7062–7067.
102 F. Wang, W. Sun, Z. Shadike, E. Hu, X. Ji, T. Gao, X. Yang, K. Xu and C. Wang, *Angew. Chem.*, 2018, **130**, 12154–12157.
103 K. Zhu, Z. Sun, P. Liu, H. Li, Y. Wang, K. Cao and L. Jiao, *J. Energy Chem.*, 2021, **63**, 239–245.
104 Z. Wu, C. Lu, F. Ye, L. Zhang, L. Jiang, Q. Liu, H. Dong, Z. Sun and L. Hu, *Adv. Funct. Mater.*, 2021, **31**, 1–12.
105 K. Zhu, Z. Sun, P. Liu, H. Li, Y. Wang, K. Cao and L. Jiao, *J. Energy Chem.*, 2021, **63**, 239–245.
106 Z. Jian, W. Han, X. Lu, H. Yang, Y. S. Hu, J. Zhou, Z. Zhou, J. Li, W. Chen, D. Chen and L. Chen, *Adv. Energy Mater.*, 2013, **3**, 156–160.
107 L. Wang and J. Zheng, *Mater. Today Adv.*, 2020, **7**, 100078.
108 Y. Marcus, *Chem. Rev.*, 1988, **88**, 1475–1498.
109 G. Li, Z. Yang, Y. Jiang, C. Jin, W. Huang, X. Ding and Y. Huang, *Nano Energy*, 2016, **25**, 211–217.
110 S. Pavithra, K. Pramoda and R. S. Keri, *Chem. Eng. J.*, 2024, **495**, 153423.
111 X. Guo, G. Fang, W. Zhang, J. Zhou, L. Shan, L. Wang, C. Wang, T. Lin, Y. Tang and S. Liang, *Adv. Energy Mater.*, 2018, **8**, 1–7.
112 F. Wan, L. Zhang, X. Dai, X. Wang, Z. Niu and J. Chen, *Nat. Commun.*, 2018, **9**, 1–11.
113 P. He, M. Yan, G. Zhang, R. Sun, L. Chen, Q. An and L. Mai, *Adv. Energy Mater.*, 2017, **7**, 1–5.
114 H. Qin, Z. Yang, L. Chen, X. Chen and L. Wang, *J. Mater. Chem. A*, 2018, **6**, 23757–23765.
115 S. Liu, X. Chen, Q. Zhang, J. Zhou, Z. Cai and A. Pan, *ACS Appl. Mater. Interfaces*, 2019, **11**, 36676–36684.

116 Y. Rong, H. Chen, J. Wu, Z. Yang, L. Deng and Z. Fu, *Ind. Eng. Chem. Res.*, 2021, **60**, 8649–8658.
117 G. Zampardi and F. La Mantia, *Curr. Opin. Electrochem.*, 2020, **21**, 84–92.
118 M. B. Zakaria and T. Chikyow, *Coord. Chem. Rev.*, 2017, **352**, 328–345.
119 J. Liu, Z. Shen and C. Z. Lu, *J. Mater. Chem. A*, 2024, **12**, 2647–2672.
120 L. Zhang, L. Chen, X. Zhou and Z. Liu, *Adv. Energy Mater.*, 2015, **5**, 1–5.
121 F. Scholz and A. Dostal, *Angew. Chem., Int. Ed. Engl.*, 1996, **34**, 2685–2687.
122 K. Hurlbutt, S. Wheeler, I. Capone and M. Pasta, *Joule*, 2018, **2**, 1950–1960.
123 J. Yang, W. Hou, L. Ye, G. Hou, C. Yan and Y. Zhang, *Small*, 2024, **20**, 1–9.
124 X. Y. Fu, L. L. Zhang, C. C. Wang, H. Bin Sun and X. L. Yang, *Rare Met.*, 2024, **44**, 34–59.
125 H. Cui, L. Ma, Z. Huang, Z. Chen and C. Zhi, *SmartMat*, 2022, **3**, 565–581.
126 Z. Tie and Z. Niu, *Angew. Chem., Int. Ed.*, 2020, **59**, 21293–21303.
127 Y. Liang, Z. Tao and J. Chen, *Adv. Energy Mater.*, 2012, **2**, 742–769.
128 Z. Tie and Z. Niu, *Angew. Chem., Int. Ed.*, 2020, **59**, 21293–21303.
129 X. Deng, J. K. Sarpong, G. Zhang, J. Hao, X. Zhao, L. Li, H. Li, C. Han and B. Li, *InfoMat*, 2023, **5**, 1–21.
130 L. Mei, J. Xu, Z. Wei, H. Liu, Y. Li, J. Ma and S. Dou, *Small*, 2017, **13**, 1–11.
131 M. M. Huie, D. C. Bock, E. S. Takeuchi, A. C. Marschilok and K. J. Takeuchi, *Coord. Chem. Rev.*, 2015, **287**, 15–27.
132 E. Levi, E. Lancry, A. Mitelman, D. Aurbach, G. Ceder, D. Morgan and O. Isnard, *Chem. Mater.*, 2006, **18**, 5492–5503.
133 A. Elgendy, A. A. Papaderakis, A. Ejigu, K. Helmbrecht, B. F. Spencer, A. Groß, A. S. Walton, D. J. Lewis and R. A. W. Dryfe, *Nanoscale*, 2024, **16**, 13597–13612.
134 X. Jia, C. Liu, Z. G. Neale, J. Yang and G. Cao, *Chem. Rev.*, 2020, **120**, 7795–7866.
135 M. Liu, G. Lv, T. Liu, H. Liu, L. Kong, L. Tian, W. Rao, Y. Li, L. Liao and J. Guo, *Prog. Nat. Sci.:Mater. Int.*, 2023, **33**, 8–15.
136 M. S. Chae, J. W. Heo, S. C. Lim and S. T. Hong, *Inorg. Chem.*, 2016, **55**, 3294–3301.
137 Y. Wei, P. Zhang, R. A. Soomro, Q. Zhu and B. Xu, *Adv. Mater.*, 2021, **33**, 1–30.
138 P. Ma, D. Fang, Y. Liu, Y. Shang, Y. Shi and H. Y. Yang, *Adv. Sci.*, 2021, **8**, 1–25.
139 M. Shekhirev, C. E. Shuck, A. Sarycheva and Y. Gogotsi, *Prog. Mater. Sci.*, 2021, **120**, 100757.
140 H. Liu, Z. Xin, B. Cao, B. Zhang, H. J. Fan and S. Guo, *Adv. Sci.*, 2024, **11**, 1–18.
141 M. Li, X. Li, G. Qin, K. Luo, J. Lu, Y. Li, G. Liang, Z. Huang, J. Zhou, L. Hultman, P. Eklund, P. O. Å. Persson, S. Du, Z. Chai, C. Zhi and Q. Huang, *ACS Nano*, 2021, **15**, 1077–1085.
142 M. Shi, B. Wang, C. Chen, J. Lang, C. Yan and X. Yan, *J. Mater. Chem. A*, 2020, **8**, 24635–24644.
143 M. S. Javed, A. Mateen, S. Ali, X. Zhang, I. Hussain, M. Imran, S. S. A. Shah and W. Han, *Small*, 2022, **18**, 1–39.
144 R. Zhao, C. Liu, Y. Zhu, G. Zou, H. Hou and X. Ji, *Adv. Funct. Mater.*, 2024, **34**, 1–28.
145 Q. Li, Y. Zhao, F. Mo, D. Wang, Q. Yang, Z. Huang, G. Liang, A. Chen and C. Zhi, *EcoMat*, 2020, **2**, 1–14.
146 X. Li, X. Ma, Y. Hou, Z. Zhang, Y. Lu, Z. Huang, G. Liang, M. Li, Q. Yang, J. Ma, N. Li, B. Dong, Q. Huang, F. Chen, J. Fan and C. Zhi, *Joule*, 2021, **5**, 2993–3005.
147 N. Zhang, F. Cheng, J. Liu, L. Wang, X. Long, X. Liu, F. Li and J. Chen, *Nat. Commun.*, 2017, **8**, 1–9.
148 J. Zhou, L. Shan, Z. Wu, X. Guo, G. Fang and S. Liang, *Chem. Commun.*, 2018, **54**, 4457–4460.
149 F. Cui, J. Zhao, D. Zhang, Y. Fang, F. Hu and K. Zhu, *Chem. Eng. J.*, 2020, **390**, 124118.
150 Z. Jia, B. Wang and Y. Wang, *Mater. Chem. Phys.*, 2015, **149–150**, 601–606.
151 Q. Zhao, W. Huang, Z. Luo, L. Liu, Y. Lu, Y. Li, L. Li, J. Hu, H. Ma and J. Chen, *Sci. Adv.*, 2018, **4**, eaao1761.
152 D. Kundu, P. Oberholzer, C. Glaros, A. Bouzid, E. Tervoort, A. Pasquarello and M. Niederberger, *Chem. Mater.*, 2018, **30**, 3874–3881.
153 T. Chen, X. Zhu, X. Chen, Q. Zhang, Y. Li, W. Peng, F. Zhang and X. Fan, *J. Power Sources*, 2020, **477**, 228652.
154 X. Li, M. Li, Q. Yang, H. Li, H. Xu, Z. Chai, K. Chen, Z. Liu, Z. Tang, L. Ma, Z. Huang, B. Dong, X. Yin, Q. Huang and C. Zhi, *ACS Nano*, 2020, **14**, 541–551.
155 Z. Xu, X. Li, Y. Jin, Q. Dong, J. Ye, X. Zhang and Y. Qian, *Nanoscale*, 2022, **14**, 11655–11663.
156 H. Zheng, Y. Huang, J. Xiao, W. Zeng, X. Li, X. Li, M. Wang and Y. Lin, *Chem. Eng. J.*, 2023, **468**, 143834.
157 H. Cao, X. Huang, Y. Li, Y. Liu, Q. Zheng, Y. Huo, R. Zhao, J. Zhao and D. Lin, *Chem. Eng. J.*, 2023, **455**, 140538.
158 B. Raza, A. Naveed, J. Chen, H. Lu, T. Rasheed, J. Yang, Y. NuLi and J. Wang, *Energy Stor. Mater.*, 2022, **46**, 523–534.
159 G. Ni, G. Zou, M. Sun, F. Xu, Z. Pan, F. Cao and C. Zhou, *ACS Appl. Energy Mater.*, 2022, **5**, 12437–12447.
160 L. Geng, J. Meng, X. Wang, C. Han, K. Han, Z. Xiao, M. Huang, P. Xu, L. Zhang, L. Zhou and L. Mai, *Angew. Chem., Int. Ed.*, 2022, **61**, 1–9.
161 C. Meng, W. He, Z. Kong, Z. Liang, H. Zhao, Y. Lei, Y. Wu and X. Hao, *Chem. Eng. J.*, 2022, **450**, 138265.
162 T. Zhang, Y. Tang, S. Guo, X. Cao, A. Pan, G. Fang, J. Zhou and S. Liang, *Energy Environ. Sci.*, 2020, **13**, 4625–4665.
163 Z. Chen, F. Mo, T. Wang, Q. Yang, Z. Huang, D. Wang, G. Liang, A. Chen, Q. Li, Y. Guo, X. Li, J. Fan and C. Zhi, *Energy Environ. Sci.*, 2021, **14**, 2441–2450.
164 W. Kao-ian, M. T. Nguyen, T. Yonezawa, R. Pornprasertsuk, J. Qin, S. Siwamogsatham and S. Kheawhom, *Mater. Today Energy*, 2021, **21**, 100738.
165 A. Naveed, H. Yang, Y. Shao, J. Yang, N. Yanna, J. Liu, S. Shi, L. Zhang, A. Ye, B. He and J. Wang, *Adv. Mater.*, 2019, **31**, 1–9.
166 Y. Mei, Y. Liu, W. Xu, M. Zhang, Y. Dong and J. Qiu, *Chem. Eng. J.*, 2023, **452**, 139574.
167 W. Bin Tu, S. Liang, L. N. Song, X. X. Wang, G. J. Ji and J. J. Xu, *Adv. Funct. Mater.*, 2024, **34**, 1–11.

168 S. Liu, W. Liu, D. Ba, Y. Zhao, Y. Ye, Y. Li and J. Liu, *Adv. Mater.*, 2023, **35**, 1–23.
169 X. Wang, X. Li, H. Fan and L. Ma, *Nano-Micro Lett.*, 2022, **14**, 1–24.
170 S. Lei, Z. Liu, C. Liu, J. Li, B. Lu, S. Liang and J. Zhou, *Energy Environ. Sci.*, 2022, **15**, 4911–4927.
171 Z. Chen, X. Li, D. Wang, Q. Yang, L. Ma, Z. Huang, G. Liang, A. Chen, Y. Guo, B. Dong, X. Huang, C. Yang and C. Zhi, *Energy Environ. Sci.*, 2021, **14**, 3492–3501.
172 L. Ma, S. Chen, X. Li, A. Chen, B. Dong and C. Zhi, *Angew. Chem., Int. Ed.*, 2020, **59**, 23836–23844.
173 F. Bu, C. Li, Q. Wang and X. Liu, *Chem. Eng. J.*, 2022, **449**, 137710.
174 P. D. Kimilita, M. Hayashi, H. M. Nkomba, H. Fukunishi, N. Lobo, T. Mizuno, L. E. Eale and E. K. Mwilambwe, *Electrochim. Acta*, 2023, **462**, 142702.
175 Y. Wang, Q. Li, H. Hong, S. Yang, R. Zhang, X. Wang, X. Jin, B. Xiong, S. Bai and C. Zhi, *Nat. Commun.*, 2023, **14**, 1–10.
176 W. Qiu, Y. Tian, Z. Lin, S. Lin, Z. Geng, K. Huang, A. Lei, F. Huang, H. Feng, F. Ding, Y. Li and X. Lu, *J. Energy Chem.*, 2022, **70**, 283–291.
177 L. Ma, S. Chen, N. Li, Z. Liu, Z. Tang, J. A. Zapien, S. Chen, J. Fan and C. Zhi, *Adv. Mater.*, 2020, **32**, 1–10.
178 Z. Zhao, J. Wang, Z. Lv, Q. Wang, Y. Zhang, G. Lu, J. Zhao and G. Cui, *Chem. Eng. J.*, 2021, **417**, 128096.
179 H. Dong, J. Li, S. Zhao, F. Zhao, S. Xiong, D. J. L. Brett, G. He and I. P. Parkin, *J. Mater. Chem. A*, 2020, **8**, 22637–22644.
180 N. Sun, H. Sun, D. Tan, Q. Guo, Z. Zhang, Z. Tao, C. Fang, J. Bu, J. Huang and C. Jiang, *Chem. Eng. J.*, 2023, **469**, 143997.
181 B. Sun, Y. Zong, K. Bao, M. Wang, P. Wang, H. Xu and Y. Jin, *ACS Appl. Mater. Interfaces*, 2023, **15**, 37916–37924.
182 R. Puttaswamy, Z. Tian, H. Lee, D. Y. Kim, A. Le Mong and D. Kim, *J. Mater. Chem. A*, 2023, **11**, 14075–14085.
183 G. Fang, S. Liang, Z. Chen, P. Cui, X. Zheng, A. Pan, B. Lu, X. Lu and J. Zhou, *Adv. Funct. Mater.*, 2019, **29**, 1–9.
184 W. Du, J. Xiao, H. Geng, Y. Yang, Y. Zhang, E. H. Ang, M. Ye and C. C. Li, *J. Power Sources*, 2020, **450**, 227716.
185 Y. Liang, Y. Jing, S. Gheytani, K. Y. Lee, P. Liu, A. Facchetti and Y. Yao, *Nat. Mater.*, 2017, **16**, 841–848.
186 Y. Wang, C. Wang, Z. Ni, Y. Gu, B. Wang, Z. Guo, Z. Wang, D. Bin, J. Ma and Y. Wang, *Adv. Mater.*, 2020, **32**, 1–8.
187 Z. Guo, Y. Ma, X. Dong, J. Huang, Y. Wang and Y. Xia, *Angew. Chem.*, 2018, **130**, 11911–11915.
188 M. Zhang, R. Liang, T. Or, Y. P. Deng, A. Yu and Z. Chen, *Small Struct.*, 2021, **2**, 1–21.
189 F. Wan, L. Zhang, X. Wang, S. Bi, Z. Niu and J. Chen, *Adv. Funct. Mater.*, 2018, **28**, 1–8.
190 B. Kaur, D. Maity, P. Y. Naidu and M. Deepa, *Chem. Eng. J.*, 2023, **468**, 143835.
191 Z. Wang, Z. Ruan, W. S. Ng, H. Li, Z. Tang, Z. Liu, Y. Wang, H. Hu and C. Zhi, *Small Methods*, 2018, **2**, 1–8.
192 X. Cai, Y. Liu, J. Zha, F. Tan, B. Zhang, W. Yan, J. Zhao, B. Lu, J. Zhou and C. Tan, *Adv. Funct. Mater.*, 2023, **33**, 1–11.
193 W. Yan, X. Cai, F. Tan, J. Liang, J. Zhao and C. Tan, *Chem. Commun.*, 2023, **59**, 1661–1664.
194 J. Yan, E. H. Ang, Y. Yang, Y. Zhang, M. Ye, W. Du and C. C. Li, *Adv. Funct. Mater.*, 2021, **31**, 1–30.
195 Y. A. Kumar, S. Vignesh, T. Ramachandran, A. M. Fouda, H. H. Hegazy, M. Moniruzzaman and T. H. Oh, *J. Ind. Eng. Chem.*, 2025, **145**, 191–215.
196 T. Ramachandran, R. K. Raji, S. Palanisamy, N. Renuka and K. Karuppasamy, *J. Ind. Eng. Chem.*, 2025, **145**, 144–168.
197 T. Ramachandran, N. Roy, H. H. Hegazy, I. S. Yahia, Y. A. Kumar, M. Moniruzzaman and S. W. Joo, *J. Alloys Compd.*, 2025, **1010**, 112478.
198 T. Ramachandran, H. Butt, L. X. Zheng and M. Rezeq, *J. Energy Storage*, 2024, **99**, 113425.